

Accepted Manuscript

Developing pyridazine-3-carboxamides to be CB2 agonists: The design, synthesis, structure-activity relationships and docking studies

Hai-Yan Qian, Zhi-Long Wang, Xiao-Yu Xie, You-Lu Pan, Gang-Jian Li, Xin Xie, Jian-Zhong Chen



PII: S0223-5234(17)30431-2

DOI: [10.1016/j.ejmech.2017.05.060](https://doi.org/10.1016/j.ejmech.2017.05.060)

Reference: EJMECH 9490

To appear in: *European Journal of Medicinal Chemistry*

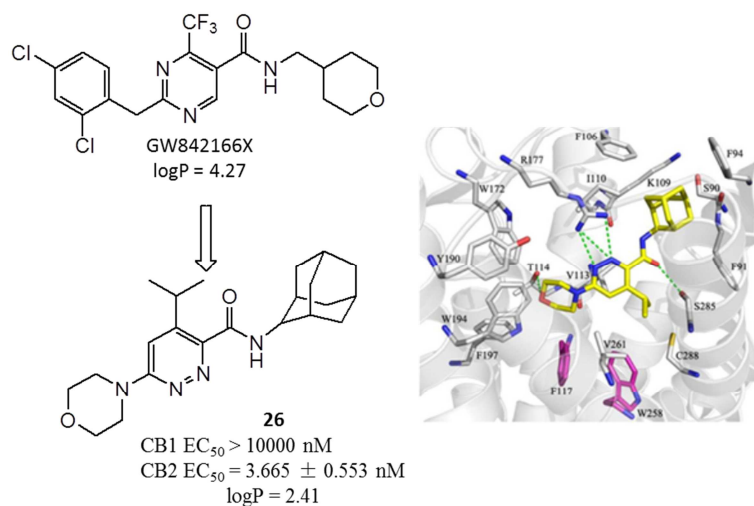
Received Date: 16 March 2017

Revised Date: 26 May 2017

Accepted Date: 29 May 2017

Please cite this article as: H.-Y. Qian, Z.-L. Wang, X.-Y. Xie, Y.-L. Pan, G.-J. Li, X. Xie, J.-Z. Chen, Developing pyridazine-3-carboxamides to be CB2 agonists: The design, synthesis, structure-activity relationships and docking studies, *European Journal of Medicinal Chemistry* (2017), doi: 10.1016/j.ejmech.2017.05.060.

This is a PDF file of an unedited manuscript that has been accepted for publication. As a service to our customers we are providing this early version of the manuscript. The manuscript will undergo copyediting, typesetting, and review of the resulting proof before it is published in its final form. Please note that during the production process errors may be discovered which could affect the content, and all legal disclaimers that apply to the journal pertain.



Novel pyridazine-3-carboxamide derivatives have been synthesized and biologically evaluated. The results show that the compound **26** has a good agonist activity and high selectivity for CB2. Docking simulations were performed to predict the receptor-agonist interactions.

**Developing pyridazine-3-carboxamides to be CB2 agonists: The design, synthesis,
structure-activity relationships and docking studies**

Hai-Yan Qian^{a, §}, Zhi-Long Wang^{b, §}, Xiao-Yu Xie^a, You-Lu Pan^a, Gang-Jian Li^a, Xin Xie^{b,*},

Jian-Zhong Chen^{a,*}

^a *College of Pharmaceutical Sciences, Zhejiang University, Hangzhou, Zhejiang 310058,
China*

^b *CAS Key Laboratory of Receptor Research, National Center for Drug Screening, Shanghai
Institute of Materia Medica, Chinese Academy of Sciences, Shanghai 201203, China*

§ These authors contributed equally.

* Corresponding Authors:

E-mail: xxie@simm.ac.cn, Tel.(Fax): 86-21-50801313 (X. Xie)

E-mail: chjz@zju.edu.cn, Tel.(Fax): 86-571-88208659 (J.-Z. Chen)

ABSTRACT

Herein, we described the design and synthesis of a series of pyridazine-3-carboxamides to be CB2-selective agonists via a combination of scaffold hopping and bioisosterism strategies. The compounds were subjected to assessment of their potential activities through calcium mobilization assays. Among the tested derivatives, more than half of these compounds exhibited moderate to potent CB2 agonist activity. Six compounds showed EC₅₀ values below 35 nM, and several derivatives also exhibited significantly enhanced potency and high selectivity at the CB2 receptor over the CB1 receptor. Specifically, compound **26** showed the highest CB2 agonist activity (EC₅₀ = 3.665 ± 0.553 nM) and remarkable selectivity (Selectivity Index > 2729) against CB1. In addition, logPs of some representative compounds were measured to display significantly decreased values in comparison with GW842166X. Furthermore, docking simulations were conducted to explain the interaction mode of this series.

Keywords:

Pyridazine-3-carboxamides, CB2 agonist, structure-activity relationships, molecular docking, logP

1. Introduction

The endocannabinoid system is composed of a group of lipid-based mediators, relative targets involved in a variety of synthesizing and metabolizing enzymes, and transporter receptors [1]. There are two G-protein coupled receptors (GPCRs), cannabinoid receptor 1 (CB1) [2] and cannabinoid receptor 2 (CB2) [3], in the endocannabinoid system. These two GPCRs share sequence homology of 44% identity at the protein level and 68% similarity in the seven transmembrane domains [4]. CB1, expressed mainly in the central nervous system (CNS) [5], has been reported to mitigate numerous pathologies [4, 6], and its ligands have been proposed for therapeutic use [7]. However, psychotropic side effects induced by the CB1 ligands limit their pharmaceutical applications. For example, CB1 antagonist SR141716A (**1**, Figure 1) was approved to be an anti-obesity agent in 2006, but withdrawn from European market two years later for its serious psychopathic side effects related to the inhibition of CB1 in the brain. After that, other CB1 antagonists, like MK-0364 (Taranabant) and CP-945598 (Otenabant), were stopped in the clinical phase studies for the same reason [8]. On the other hand, CB2 is found predominantly in the periphery [9], particularly in the immune and skeletal systems [10, 11]. Pharmacological studies have demonstrated that CB2 ligands exhibit marvelously therapeutic potentials in the treatment of different pathologies, including immune-related disorders [12], pain [13], inflammation [14], osteoporosis [15], neuro-degeneration [16], and cancer [17]. Thus, CB2 selective ligands catch more attention in the recent years since they avoid the CNS influence by taking effects in the peripheral system.

Up to now, there were a large number of CB2 ligands reported by pharmaceutical companies or academic research laboratories [18-20]. As illustrated in Figure 1, some representatives of CB2 agonists were developed based on traditional cannabinoids, such as compounds **2** (HU-308) [21], **3** (GW405833) [22], **4** (JWH-015) [23], and **5** (AM1241) [24], while the pyrazole derivative **6** (SR144528) is a prototypical CB2 antagonist. Besides, structurally diverse compounds were also discovered to be CB2 ligands, like the CB2 inverse agonist **7** (JTE-907) [25] displaying to be effective in suppressing itch-associated responses in NC mice of atopic dermatitis without the adverse effect on the losing weight and exacerbation of dermatitis [26]. Encouragingly, there were some CB2 ligands getting into clinic trail studies [17]. For example, the CB2 agonist **8** (GW842166X, Figure 1) [27] has completed Phase II clinical trials for evaluating its analgesic efficacy in the treatment of osteoarthritic and dental pain [28]. Unfortunately, clinical trials of GW842166X failed to achieve satisfactory effects. In addition, CB2 agonist **9** (S-777469, Figure 1) was studied to exhibit moderate bioactivity and excellent selectivity for the CB2 receptor [29]. Pharmacological studies suggested that S-777469 had a significant antipruritic efficiency in the pruritic animal model, and displayed standout metabolism and pharmacokinetic properties [30]. It has also been reported on completing its phase II clinical trials for allergic contact dermatitis [31]. However, there is no relevant CB2 ligand approved for market. One of reasons is probably their relatively high lipophilicity to induce inadequate drug-likeness.. The high lipophilicity of CB2 ligands may be a key factor for CB2 ligands not showing optimal pharmacokinetic profile, like high binding to plasma proteins, long half-life, low bioavailability and off-target effects [32]. As we measured, logP value of GW842166X was

4.27 [33]. The logP was recognized to be the important drug-likeness property for a bioactive compound to be developed as therapeutic agent. Reducing logP could be a strategy for CB2 ligands to have desired pharmacokinetic properties [34].

In the previous reports, GW842166X (Figure 1) was demonstrated to possess high potency, efficacy, and selectivity due to low molecular weight and polar surface area, despite its low aqueous solubility [35]. The aforementioned facts motivated us to investigate new aromatic core with improved aqueous solubility. In this context, bioisosterism strategy was applied for designing pyridazine-3-carboxamides as CB2 agonists by replacing the central pyrimidine core of GW842166X with a pyridazine nucleus, since the basic pK_a of pyridazine (2.33) is higher than pyrimidine (1.3) and pyridazine showed measurable aqueous solubility, which could be improved through salt formation [36]. Based on critical pharmacophore features predicted by our docking-simulated interaction mode of GW842166X binding to the CB2 receptor (Figure S1 in the Supporting Information), we designed and synthesized a series of pyridazine-3-carboxamides (general structure A, Figure 1). The structural pieces suggested good alignment with pharmacophoric features of GW842166X. The cell-based calcium mobilization assays [37] were used to evaluate *in vitro* functional activities of synthesized pyridazine-3-carboxamide derivatives. Structure-activity relationships (SARs) studies were mainly performed on the substituent (R_1) on the pyridazine nucleus, the C-3 amide groups (R_2), and the C-6 substituent group (R_3). The bioactive tests indicated that the synthesized compounds displayed good agonist activity towards CB2 and high selectivity against CB1, and some compounds showed much higher potency in relative to GW842166X. Finally, molecular docking simulations were carried out with the aim of understanding the structural

requirements for new derivatives binding to the CB2 receptor.

2. Chemistry

The synthetic route for the target pyridazine-3-carboxamide derivatives **21-55** was depicted in Scheme 1. The structures of pyridazine-3-carboxamide derivatives were confirmed by ^1H NMR, ^{13}C NMR spectrum, and mass spectrometry.

As shown in Scheme 1, the commercially available material α -ketoglutaric acid **10** was converted into the 6-oxo-1,4,5,6-tetrahydropyridazine-3-carboxylic acid **11** upon treatment with hydrazine sulfate in the presence of sodium hydroxide in water. In the next step, acid-catalyzed enol formation, bromination, and elimination of HBr, provided 6-oxo-1,6-dihydropyridazine-3-carboxylic acid **12** [38]. Analogously to the reported procedures [39, 40], **12** was subsequently submitted to chlorination using thionyl chloride to give the corresponding acid chloride **13**, and then reacted with diverse primary amines to afford the amide analogs **14a-14c**. Subsequent nucleophilic substitution of the key intermediates **14a-14c** with morpholine provided the final pyridazine-3-carboxamide derivatives **21-23**.

On the other hand, treatment of the intermediate **12** by refluxing in ethanol of hydrogen chloride led to the ethyl 6-oxo-1,6-dihydropyridazine-3-carboxylate **15**, and which was subsequently reacted with phosphorus oxychloride to yield the ethyl 6-chloropyridazine-3-carboxylate **16** [41]. Successively, compound **16** was then subjected to Minisci Reaction with homolytic alkylation by free isopropyl radical, generated by silver-catalyzed oxidative decarboxylation of isobutyric acid, and led to a mixture (ca 1:10 regioisomeric ratio) of regioisomers **17a** and **17b** that were separated by flash chromatography on silica gel column

[42]. The two regioisomers **17a** and **17b** were identified on the basis of the chemical shifts of the aromatic protons (shown in the Supporting Information). Furthermore, it has been reported that similar pyridazines with a carbonitrile group instead of the ethyl ester function reacted with pivalic acid under the same conditions to obtain a 3:7 mixture of two regioisomers, and the major component confirmed by X-ray analysis, having the same regiochemistry of our synthesized intermediate **17b** [43]. Compounds **17a** and **17b** afforded the corresponding carboxylic acids **18a** and **18b**, respectively, through the alkaline hydrolysis with lithium hydroxide in good overall yields. The key intermediates **20a-20f** were obtained according to the above procedures that were utilized for preparing the amide analogs **14a-14c**, by refluxing the newly formed **18a-18b** with thionyl chloride, and then distilling off the excess reagent to afford the crude acid chlorides **19a-19b**. Afterwards, treatment of **19a-19b** with the suitable primary amines in the presence of triethylamine eventually gave the amide derivatives **20a-20f** in moderate to good yield. Finally, the targeted compounds **24-53** were produced via the reaction between the compounds **20a-20f** and the aromatic amines in acetonitrile heated to 160 °C [44] or the aliphatic amines in 1,4-dioxane at reflux temperature [39].

3. Results and discussion

3.1. *In vitro* biological evaluations

All the synthesized compounds were evaluated *in vitro* for their functional activities by using our developed cell-based calcium mobilization assays [37]. Both GW842166X and JTE-907 were included in the experiments as the reference standards of CB2 agonist and

antagonist, respectively. Two commercially available ligands, CP55940 and SR141716A were used as positive controls for agonist mode and antagonist mode, respectively, in the bioactive assays. At first, all compounds were screened for their functional effects towards CB1 and CB2 at 10 μ M concentration, respectively, using the method described in the Supporting Information, and the results are summarized in Table S1. The initial screening results indicated that most compounds demonstrated activating bioactivity to CB2. Those compounds displaying more than 50% activation activity were further evaluated in dose-response studies to determine their EC_{50} values. As summarized in Tables 1-3, more than half of the tested compounds exhibited moderate to potent CB2 full agonist activities. Six compounds showed EC_{50} values below 35 nM for the CB2 receptor with high selectivity against CB1. Typically, compound **26** demonstrates a full agonist activity with the EC_{50} value of 3.665 ± 0.553 nM, which is 94-fold and 8-fold more potent than GW842166X and CP55940, respectively. Besides, other four compounds **36** ($EC_{50} = 5.701 \pm 1.993$ nM), **38** ($EC_{50} = 4.955 \pm 0.633$ nM), **39** ($EC_{50} = 18.08 \pm 2.89$ nM), and **42** ($EC_{50} = 17.13 \pm 1.59$ nM) display higher CB2 agonist activities and have much higher selectivity over the CB1 receptor than both GW842166X and CP55940. Moreover, it was noticed that all these potent CB2 agonists have $clogD$ values, calculated by using ACD/ADME Suite software [45] less than 5 and exhibit remarkably improved solubility in comparison with GW842166X.

The $\log S$ for pyridazine-3-carboxamide derivatives **21-55** along with GW842166X and CP55940 were calculated using ACD/ADME Suite software [45] to predict their aqueous solubility. As listed in Tables 1-3, the predicted results reveal that all our synthesized compounds possess higher calculated $\log S_{PH7.4}$ (-1.95 ~ -4.95) compared with GW842166X

($\text{clogS}_{\text{PH}7.4} = -5.65$) and CP55940 ($\text{clogS}_{\text{PH}7.4} = -5.27$), suggesting that these newly pyridazine-3-carboxamide derivatives displayed substantially improved aqueous solubility.

The logP is an important drug-likeness property, and appropriate logP for a drug candidate was proposed to be 1 ~ 3 [46]. In order to position drug-like physicochemical properties of the synthesized compounds, four representative compounds **26**, **38**, **39**, and **42** were selected to measure their logP values using the methods described in the previous manuscript [33]. As results, these four compounds display their logP values to be 2.41, 2.01, 3.40, and 3.16, respectively, decreasing significantly in comparison with GW842166X with the measured logP value of 4.27 [33]. By structural optimization, we developed pyridazine-3-carboxamides to be CB2-selective agonists, not only showing high potency on CB2 and selectivity against CB1 but also having appropriate logP.

3.2. Structure-activity relationships

We started structure-activity relationships studies by the synthesis of a series of derivatives with various substitutions on pyridazine-3-carboxamide scaffold to investigate the impact of this variable on their activities. Among three compounds **21-23** without a substituent (R_1) on the C4- or C5-position, **21** and **22** were detected to have no bioactivity on neither CB1 nor CB2, while compound **23** showed a low CB2 agonist activity ($\text{EC}_{50} = 8425 \pm 4183$ nM). By comparing the bioactivities of compounds without a substituent (**21**, **22**, **23**) and compounds with a R_1 4-isopropyl (**24**, **25**, **26**) or 5-isopropyl (**27**, **28**, **29**), it was found that a substituent at the C-4 or C-5 site of pyridazine-3-carboxamide scaffold would be a desirable feature for improving the CB2 agonist activity. In the meantime, it was noticed that **24-26** bearing a R_1

4-isopropyl group displayed higher bioactivities than 5-isopropyl analogs **27-29**. These results revealed the crucial role of R₁ 4-isopropyl group for pyridazine-3-carboxamides to interact with CB2. By comparing the binding modes of our synthesized pyridazine-3-carboxamides with GW842166X, it could be proposed that the pyridazine core may be embraced by hydrophobic residues V113, F117, F177, W258, and V261 of the CB2 receptor. In addition, structural alignments indicated that the R₁ 4-isopropyl group of pyridazine-3-carboxamides may superimpose with the 4-CF₃ of GW842166X. Therefore, a proper hydrophobic substituent on the 4-position of pyridazine core would be benefit to have hydrophobic interactions with the CB2 receptor. Typically, **26** with R₁ 4-isopropyl, R₂ 2-adamantyl, and R₃ morpholino ring displays the highest CB2 bioactivity (EC₅₀ = 3.665 ± 0.553 nM) and selectivity against CB1 among all of the synthesized pyridazine-3-carboxamides.

Moreover, it was predicted that the amide moiety of GW842166X might lie deeply in a hydrophobic sub-pocket embraced by the residues F91, F94, F106, K109, and I110 (Figure S1 in the Supporting Information), so a modest steric hindrance adjacent to the amide would be a preferred building block for the CB2 agonist activity of pyridazine-3-carboxamides. This hypothesis was confirmed by the replacement of the R₂ cyclohexyl subunit with an adamantyl group, which had a significant impact on the CB2 agonist activity. Either compound **25/26** with a R₂ 1-adamantyl group or **28/29** with a R₂ 2-adamantyl group possess higher CB2 agonist activity in comparison with the corresponding compound **24** and **27** with a R₂ cyclohexyl group. Therefore, a R₂ adamantyl group was demonstrated to have more positive impact on the CB2 agonist activity of pyridazine-3-carboxamides than a R₂ cyclohexyl.

After preliminary identification of the preference for the R₁ 4-isopropyl substitution, 4-isopropylpyridazine-3-carboxamides **30-38** with diverse R₃ groups were synthesized to characterize the effect of R₂ 1-adamantyl or 2-adamantyl on the CB2 bioactivity. It was observed that EC₅₀ values increased for 4-isopropylpyridazine-3-carboxamide derivatives with the corresponding R₂ subunit in the order of cyclohexyl (**30**), 1-adamantyl (**33**), and 2-adamantyl (**36**). Similarly, this trend is also seen in other different R₃ substituted compounds, whose EC₅₀ values are decreased in the order of 2-adamantyl (**37** or **38**), 1-adamantyl (**34** or **35**), and cyclohexyl (**31** or **32**), respectively. These results further confirmed that the R₂ 2-adamantyl group would be the best choice to 4-isopropylpyridazine-3-carboxamides as CB2 agonists. Among these compounds, **36** or **38** shows the CB2 agonist activity similar to **26**. Actually, docking simulations discussed later will suggest that R₂ 2-adamantyl of **26** would have maximal hydrophobic space-filling in the pocket surrounded by the key residues F91, F94, F106, K109, and I110 (Figure 2A).

SAR studies were continued to explore the influence of R₃ units on the CB2 agonist activity of 4-isopropylpyridazine-3-carboxamides with a constant R₂ 2-adamantyl group. As shown in Table 2, compound **39** with a R₃ piperidinyl group shows more than 4-fold lower CB2 agonist activity than **26** with a R₃ morpholino, and *N*-methylpiperazin derivative **40** results in complete loss of activity. By introducing a cyclohexylamino group in place of the morpholino group of **26**, the obtained compound **41** shows more than 108-fold drop in CB2 agonist activity. However, compound **36** with a cyclopentylamino group or **42** with a cyclopropylamino group maintains CB2 agonist activity similar as **26**. In addition, either **43** with a cyclopropylmethylenamino group or **37** with an *n*-butylamino group was also

examined to be a CB2 agonist, showing 13-times lower bioactivity than **26**. Moreover, it would not be helpful to introduce a branched pentylamino chain (**44**) at the R₃ position. Furthermore, replacement of the R₃ *n*-butylamino of **37** with 2-hydroxyethylamino led to analog **38**, which has the CB2 agonist activity similar to **26**. As discussed later, docking simulations will indicate the flexible R₃ 2-hydroxyethylamino of **38** would have a similar H-bond interaction with T114 like the R₃ morpholino ring of **26** (Figure 2D). On the other hand, compound **45** with a R₃ aromatic moiety do not show potency on neither CB1 nor CB2 receptors, suggesting the R₃ aromatic substitution unfavorable for CB2 agonist activity. Herein, a modest steric hindrance or more flexible substituent at the R₃ position would be beneficial for improving CB2 agonist activity of pyridazine-3- carboxamides. Furthermore, by detecting the CB2 agonist activity of compounds **36** ($EC_{50} = 5.701 \pm 1.993$ nM) with a hydrophobic R₃ cyclopentylamino group or **38** ($EC_{50} = 4.955 \pm 0.633$ nM) with a hydrophilic R₃ 2-hydroxyethylamino group, it was found that both hydrophobicity and hydrophilicity are tolerated for R₃ substituent.

Furthermore, SAR analyses were performed to investigate the influence of R₃ substituent of 5-isopropylpyridazine-3-carboxamides on the CB2 bioactivity. As summarized in Table 3, some 5-isopropylpyridazine-3-carboxamides also display potent CB2 agonist activity, such as **48** ($EC_{50} = 34.42 \pm 2.97$ nM, $E_{max} = 114 \pm 4\%$), **51** ($EC_{50} = 96.24 \pm 17.98$ nM, $E_{max} = 93 \pm 6\%$), and **52** ($EC_{50} = 99.86 \pm 21.14$ nM, $E_{max} = 127 \pm 10\%$). As like 4-isopropylpyridazine-3-carboxamides, replacement of the R₃ morpholino group with a piperidinyl resulted in the reduced EC_{50} value by more than 8-times, as illustrated by the activity of **46** vs **29**. Whereas, both the R₃ cyclohexylamino (**47**) and cyclopropylamino (**48**) substitutions may enhance the

CB2 agonist activity in comparison with the R₃ morpholino group (**29**). In particular, **48** displays an improved bioactivity by more than 10-fold compared with GW842166X. The R₃ cyclopropylmethylenamino derivative **49** shows a decrease in the CB2 agonist activity than **48**. Moreover, the R₃ *n*-butylamino substituted analog **50** displays 3-times lower bioactivity than **48**. In addition, there is an apparent decrease in CB2 selectivity on compounds **49** and **50** owing to their CB1 agonist activity. Compound **51** with a R₃ branched pentylamino chain are inactive on both CB1 and CB2. Furthermore, the polar 2-hydroxyethylamino compound **52** was found to have more than 4-fold higher CB2 agonist activity than **29**. However, compound **55** with a R₃ 3-chlorophenylamino group is deprived of the CB2 activity. Taken together, our SAR results suggest that a R₃ group with appropriate steric hindrance is required for pyridazine-3-carboxamides to be a potent CB2 agonist. In the meantime, a substituent at C-4 position was confirmed to be a preferred for the CB2 receptor bioactivity in comparison with the C5-substitution by comparing the CB2 agonist activities of **26** vs **29**, **36** vs **48**, or **38** vs **52**, which could pave the way to develop high potency and selectivity ligands for CB2 receptor in the future.

3.3. Docking-predicted interaction modes of pyridazine-3-carboxamides binding to the CB2 receptor

In an attempt to explain how our designed compounds interact with active site of the CB2 receptor and how this relates to their CB2 agonist activities, flexible docking simulations were carried out to predict the receptor-ligand interactions by using the FlexiDock module of Sybyl-X1.3 [47]. As shown in Figure 2, Several representative compounds with different

CB2 agonist activities (**26**, **29**, **37**, and **38**) were selected to investigate the different interaction modes with the CB2 receptor on the basis of our previously generated homology model [48].

Evidently, these four typical analogs display similar binding poses but a little bit different interaction patterns (Figure 2). In each of the CB2-ligand complexes, the carbonyl group of the C-3 amide moiety conferred a critical H-bond interaction with the side chain hydroxyl group of S285. Similarly, the corresponding H-bond interaction was also observed in the binding mode of GW842166X (Figure S1 in the Supporting Information). As formerly hypothesized, the nitrogen atoms of pyridazine nucleus engaged in three H-bonds with the side chain of residue R177, suggesting that the pyridazine core would be a better choice than pyrimidine template. S285 and R177 were also proposed to play important roles in the binding of CP55940 to the CB2 receptor according to the docking and molecular dynamics simulations [49]. Docking of the most active ligand **26** showed a slightly different binding mode with other compounds (Figure 2A). In the simulated structural model of complex CB2-**26**, the polar morpholino group points to a hydrophobic pocket surrounded by the side chains of W172, Y190, W194, and F197, which had been identified as crucial residues for ligand recognition in the CB2 receptor [50-52]. Meanwhile, the oxygen atom of morpholino may form an H-bond interaction with the side chain hydroxyl group of residue T114. The bond length and angle are 2.34 Å and 160.58°, respectively. The R₂ 2-adamantyl moiety may fully occupy the hydrophobic sub-pocket composed of the side chains of the residues F91, F94, F106, K109, and I110, which indicating that a moderate bulky group is favorable at this position. For comparison, analogs **24** with a R₂ cyclohexyl and **25** with a R₂ 1-adamantyl

group were selected to study the different binding modes of agonists with CB2 receptor. A three-dimensional superposition of these three ligands in the CB2 receptor binding cavity is shown in Figure S2 in the Supporting Information. It was noted that a smaller hydrophobic cyclohexyl group of **24** would be minimally space-filling in the binding pocket. Whereas, the introduced 1-adamantyl group of **25** squeezes into the hydrophobic region adjacent to the side chains of residue F91, making **25** undergo movements to fit the binding cavity, thus reducing the interactions with R177. The tighter contact may be the major reason for the considerably decreased activity of **25**. These observations led us to think that the occupancy of this region is fundamental for a ligand.

As for docking-simulated structural model of CB2-**29** complex (Figure 2B), because of the restriction of the R₂ 5-isopropyl group, compound **29** has its R₃ morpholino group move away to miss the H-bond interaction with the residue T114. This is probably the reason for 4-isopropylpyridazine-3-carboxamides showing higher CB2 agonist activities than 5-isopropylpyridazine-3-carboxamides. For the docking-simulated CB2-**37** complex (Figure 2C), the R₃ *n*-butyl chain tightly stretches into the hydrophobic sub-pocket composed of W172, Y190, W194, and F197. the cyclopentyl group, the *n*-butyl group would be at a disadvantage in van der Waals interaction with the hydrophobic residues, inducing lower bioactivity of **37** than **36**. In the simulated structural model of complex CB2-**38** (Figure 2D), **38** with a polar 2-hydroxyethylamino as the R₃ group displays similar receptor-ligand interaction as that of the complex CB2-**26**. The hydroxyl oxygen atom of **38** may also serve as an H-bond receptor for residue T114. As for bioactivity assays data, both **26** and **38** compounds showed potent CB2 agonist activities. Consequently, the H-bond interaction with

the side chain hydroxyl group of T114 would be beneficial for the CB2 bioactivity of pyridazine-3-carboxamides.

Furthermore, the core ring of these compounds contacts with the side chains of residues V113, F117, W258, V261, and C288. In the docking-simulated model of CB2-GW842166X, the aromatic side chains of residues F117 (3.36) and W258 (6.48) of CB2 may form a parallel π - π interaction with a distance of 5.07 Å. Previous studies have revealed that the F3.36/W6.48 interaction may be the rotamer toggle switch for the protein activation [49, 53, 54]. In the docking-simulated structural models of four complexes, our docking results are congruent with the predicted interaction mode between CB2 and the GW842166X, which has the W258's side chain indole ring to maintain the parallel π - π interactions with the side chain aromatic ring of F117. Overall, these effects are consistent with their activity data.

4. Conclusion

In summary, we have described the synthesis and biological evaluation of pyridazine-3-carboxamide derivatives as novel CB2-selective agonists. Most of these compounds exhibit moderate to potent CB2 agonist activity and high selectivity against the CB1 receptor. Among these derivatives, six compounds were confirmed as potent CB2 agonists with EC_{50} values below 35 nM. Especially, compound **26** showed the highest CB2 agonist activity with an EC_{50} value of 3.665 ± 0.553 nM and remarkable selectivity index of more than 2729 over the CB1 receptor. The SAR analyses revealed that a R_1 group at C-4 position, a hydrophobic R_2 moiety with 2-adamantyl substituent, and a R_3 steric moderate aliphatic group would be favorable to the CB2 agonist activity of pyridazine-3-carboxamides.

In addition, molecular docking simulations were carried out to predict their plausible binding modes and corresponding interaction patterns with the key residues around the active site of the CB2 receptor. The docking results suggested that pyridazine-3-carboxamides share similar receptor-ligand interactions like that of GW842166X. Taken together, novel series of pyridazine-3-carboxamide derivatives and molecular docking simulations could provide a viable starting point for the development of potent CB2 agonists and give a guideline for further structural optimization.

5. Experimental section

5.1. Compound syntheses

5.1.1. Materials and instrumentation

All reactions involving air or moisture-sensitive compounds were performed under nitrogen atmosphere and reaction progress was monitored by thin-layer chromatography (TLC) on silica gel plates (GF254). Column chromatography was performed using silica gel 200-300 mesh. Melting points were measured with a Büchi Melting Point B-540 apparatus (Büchi Labortechnik, Flawil, Switzerland). ^1H NMR and ^{13}C NMR spectra were recorded on 500 MHz and 125 MHz instruments (Bruker Bioscience, Billerica, MA, USA), respectively, with TMS as an internal standard. The values of chemical shifts (δ) were given in ppm and coupling constants (J) in Hz. The abbreviations used to characterize the signals are as follows: s (singlet), d (doublet), t (triplet), q (quartet), m (multiplet), dd (doublet of doublet), *etc.* Mass spectra (MS) were taken in ESI mode on Agilent 1100 LC-MS (Agilent, Palo Alto, CA, USA). Dichloromethane (DCM), 1,2-dichloroethane and *N,N*-dimethylformamide (DMF) were dried

by distillation from calcium hydride. Triethylamine (Et₃N) was dried by distillation from potassium hydroxide. All other solvents and reagents were purchased from commercial sources and used as received without further purification.

5.1.2. Preparation of 6-oxo-1,4,5,6-tetrahydropyridazine-3-carboxylic acid (11)

A well-stirred solution of α -ketoglutaric acid (1.14 g, 7.81 mmol) in hot water (1.8 mL) was added slowly, with stirring to a solution of sodium hydroxide (0.69 g, 17.25 mmol) and hydrazinium sulfate (1.02 g, 7.85 mmol) in hot water (4.5 mL). The mixture was heated to moderate boiling overnight, and then refrigerated in ice bath for several hours. The precipitate was collected by filtration and recrystallized with 2 N HCl to provide **11** as a colorless needle crystal (691.1 mg, yield 62.3%). Mp: 195.4-195.9 °C (Ref. melting point 195-196 °C [55]).

5.1.3. Preparation of 6-oxo-1,6-dihydropyridazine-3-carboxylic acid (12)

To a solution of **11** (568 mg, 4.00 mmol) in glacial acetic acid (2.0 mL) was vigorously stirred at slight boiling temperature, then bromine (230 μ L, 4.50 mmol) was added via dropping funnel. When all of the bromine had been introduced, water (2.0 mL) was added and the reaction mixture was heated under reflux temperature overnight. After cooling to room temperature, the precipitate was filtrated, and then dried to give crude product **12** without further purification. The average yield of acid which precipitated was 334.1 mg (60.0%). Mp: 258.4-258.6 °C (Ref. melting point 257 °C [55]).

5.1.4. Preparation of 6-chloropyridazine-3-carbonyl chloride (13)

Dry DMF (18 μ L), thionyl chloride (250 μ L, 3.52 mmol), and dry 1,2-dichloroethane (2.5 mL) was added to 6-oxo-1,6-dihydropyridazine-3-carboxylic acid **12** (100 mg, 0.72 mmol), and the mixture was heated at 68 °C overnight. After completion, the excess solvent was

concentrated *in vacuo*, and the crude product of acyl chloride **13** was used immediately without further purification.

5.1.5. General procedures for the preparation of amide analogues 14a-14c

Amine (1.08 mmol) and triethylamine (1.44 mmol) were added to dry DCM (5.4 mL) at ice bath in another flask, and the newly synthesized acyl chloride **13** was dissolved in dry DCM (2.5 mL) and added dropwise via dropping funnel. The mixture was stirred at room temperature overnight. The resultant was poured into cooled water, and the organic layer was washed with 1 N HCl, saturated NaHCO₃ aqueous solution, and saturated NaCl aqueous solution, dried over anhydrous MgSO₄, and evaporated *in vacuo*. The residue was purified by flash chromatography on silica gel (200-300 mesh, hexane: ethyl acetate = 8:1 to 5:1) to obtain the compounds **14a-14c**.

5.1.5.1. 6-chloro-N-cyclohexylpyridazine-3-carboxamide (14a)

Yellow solid. Yield: 55.2%. Mp: 157.1-158.2 °C. ¹H NMR (CDCl₃, 500 MHz): δ 8.29 (d, *J* = 9 Hz, 1H), 7.94-7.96 (m, 1H), 7.68 (d, *J* = 8.5 Hz, 1H), 4.03-3.98 (m, 1H), 2.05-2.02 (m, 2H), 1.82-1.77 (m, 2H), 1.68-1.65 (m, 1H), 1.49-1.40 (m, 2H), 1.39-1.31 (m, 2H), 1.30-1.24 (m, 1H). MS (ESI), *m/z*: 240.12 [M+H]⁺.

5.1.5.2. N-(adamantan-1-yl)-6-chloropyridazine-3-carboxamide (14b)

Yellow solid. Yield: 50.4%. Mp: 200.8-202.1 °C. ¹H NMR (CDCl₃, 500 MHz): δ 8.25 (d, *J* = 8.5 Hz, 1H), 7.86 (s, 1H), 7.66 (d, *J* = 8.5 Hz, 1H), 2.16 (s, 9H), 1.78-1.72 (m, 6H). MS (ESI), *m/z*: 292.13 [M+H]⁺.

5.1.5.3. N-(adamantan-2-yl)-6-chloropyridazine-3-carboxamide (14c)

Yellow solid. Yield: 51.6%. Mp: 171.2-172.5 °C. ¹H NMR (CDCl₃, 500 MHz): δ 8.46 (d, *J*

= 5 Hz, 1H), 8.29 (d, $J = 8.5$ Hz, 1H), 7.69 (d, $J = 8.5$ Hz, 1H), 4.30-4.28 (m, 1H), 2.08 (s, 2H), 1.97 (d, $J = 13.5$ Hz, 2H), 1.92 (s, 6H), 1.80 (s, 2H), 1.72 (d, $J = 13$ Hz, 2H). MS (ESI), m/z : 292.13 $[M+H]^+$.

5.1.6. Preparation of ethyl 6-oxo-1,6-dihydropyridazine-3-carboxylate (**15**)

A solution of **12** (1.11 g, 7.92 mmol) in 8 mL of hydrogen chloride in ethanol (hydrogen chloride gas generated by reacting sodium chloride with concentrated sulfuric acid was passed into ethanol in an ice bath) was reflux for 14 h. After cooling to room temperature, the precipitate was filtered off and dried to give **15** as a white solid (1.17 g, yield 87.5%). Mp: 125.0-125.8 °C (Ref. melting point 127-128 °C [56]).

5.1.7. Preparation of ethyl 6-chloropyridazine-3-carboxylate (**16**)

A solution of **15** (1.17 g, 6.96 mmol) in phosphorus oxychloride (12 mL) was heated at 100 °C for 2 h. After cooling, the solution was concentrated *in vacuo* to 3 mL, and the residue was carefully poured into ice water, slowly neutralized with 10% NaOH aqueous solution in ice bath, and then extracted with ethyl acetate. The organic layer was washed with saturated NaCl aqueous solution, dried over anhydrous $MgSO_4$, and evaporated *in vacuo*. The residue was purified by flash chromatography on silica gel (200-300 mesh, hexane: ethyl acetate = 3:1) to obtain the compound **16** as a white solid (892 mg, yield 68.7%). Mp: 145.6-146.7 °C (Ref. melting point 154-155 °C [56]).

5.1.8. General procedures for the preparation of intermediates **17a-17b**

To a suspension of ethyl 6-chloropyridazine-3-carboxylate **16** (534 mg, 2.87 mmol) in distilled water (9 mL), isobutyric acid (60 μ L, 0.65 mmol), *conc.* H_2SO_4 (230 μ L, 4.31 mmol) and $AgNO_3$ (48.75 mg, 0.29 mmol) were added at room temperature. The mixture was heated

at 65-75 °C and a solution of $\text{NH}_4\text{S}_2\text{O}_8$ (982.40 mg, 4.31 mmol) in distilled water (5 mL) was added dropwise in 10-15 minutes. The reaction was stirred for an additional 30 minutes at 70-75 °C, then poured over ice, then neutralized with a 30% aqueous solution of NH_4OH and immediately extracted twice with dichloromethane. The collected organic layers were dried over anhydrous MgSO_4 , and evaporated *in vacuo*. The residue was purified by flash chromatography on silica gel (200-300 mesh, hexane: ethyl acetate = 5:1) to obtain the regioisomer **17a** (29.4 mg, yield 4.5%) and regioisomer **17b** (294.0 mg, 44.9%).

Ethyl 6-chloro-4-isopropylpyridazine-3-carboxylate (17a)

Yellow liquid. ^1H NMR (CDCl_3 , 500 MHz): δ 7.51 (s, 1H), 4.54-4.49 (q, 2H), 3.47-3.41 (m, 1H), 1.46 (t, $J = 7$ Hz, 3H), 1.31 (s, 3H), 1.29 (s, 3H). MS (ESI), m/z : 229.11 $[\text{M}+\text{H}]^+$.

Ethyl 6-chloro-5-isopropylpyridazine-3-carboxylate (17b)

Yellow liquid. ^1H NMR (CDCl_3 , 500 MHz): δ 8.06 (s, 1H), 4.57-4.53 (q, 2H), 3.38-3.32 (m, 1H), 1.48 (t, $J = 7$ Hz, 3H), 1.35 (s, 3H), 1.33 (s, 3H). MS (ESI), m/z : 229.10 $[\text{M}+\text{H}]^+$.

5.1.9. General procedures for the preparation of intermediates 18a-18b

To a solution of ethyl ester **17** (1 equiv.) in a 4:1 mixture of THF/ H_2O (0.05 M solution) LiOH hydrate (1.2 equiv.) was added at 0 °C. After the hydrolysis is completed (TLC monitoring), the solution was acidified carefully with a 1 N HCl, heated to room temperature and extracted with ethyl acetate. The collected organic layers were dried over anhydrous MgSO_4 , filtrated and the solvent removed under reduced pressure leading to the free carboxylic acid **18** that was used without further purification.

5.1.10. General procedures for the preparation of acyl chlorides 19a-19b

The similar procedures for the preparation of **13** were used to prepare the compounds **19a**

-19b by replacing the reactant **12** with intermediate compound **18**. The crude products of acyl chlorides **19a-19b** were used for next step.

5.1.11. General procedures for the preparation of amide analogues 20a-20f

The similar procedures for the preparation of intermediate compound **14** were used to prepare the compounds **20a-20f** by replacing the reactant **13** with intermediate compound **19**.

6-chloro-N-cyclohexyl-4-isopropylpyridazine-3-carboxamide (20a)

Yellow solid. Yield: 49.4%. Mp: 116.4-118.4 °C. ¹H NMR (CDCl₃, 500 MHz): δ 7.80 (d, *J* = 6.5 Hz, 1H), 7.54 (s, 1H), 4.33-4.27 (m, 1H), 3.98-3.91 (m, 1H), 2.05-2.01 (m, 2H), 1.80-1.76 (m, 2H), 1.68-1.64 (m, 1H), 1.47-1.38 (m, 3H), 1.36-1.31 (m, 2H), 1.29 (s, 3H), 1.28 (s, 3H). MS (ESI), m/z: 282.17 [M+H]⁺.

N-(adamantan-1-yl)-6-chloro-4-isopropylpyridazine-3-carboxamide (20b)

Yellow solid. Yield: 32.2%. Mp: 148.5-149.5 °C. ¹H NMR (CDCl₃, 500 MHz): δ 7.60 (s, 1H), 7.52 (s, 1H), 4.27-4.22 (m, 1H), 2.15 (s, 9H), 1.76-1.70 (m, 6H), 1.29 (s, 3H), 1.27 (s, 3H). MS (ESI), m/z: 334.20 [M+H]⁺.

N-(adamantan-2-yl)-6-chloro-4-isopropylpyridazine-3-carboxamide (20c)

Yellow solid. Yield: 28.2%. Mp: 118.5-120.0 °C. ¹H NMR (CDCl₃, 500 MHz): δ 8.31 (d, *J* = 7 Hz, 1H), 7.55 (s, 1H), 4.34-4.28 (m, 1H), 4.25-4.23 (m, 1H), 2.07 (s, 2H), 1.94 (d, *J* = 14 Hz, 2H), 1.91 (s, 6H), 1.78 (s, 2H), 1.70 (d, *J* = 12.5 Hz, 2H), 1.30 (s, 3H), 1.29 (s, 3H). MS (ESI), m/z: 334.19 [M+H]⁺.

6-chloro-N-cyclohexyl-5-isopropylpyridazine-3-carboxamide (20d)

White solid. Yield: 97.2%. Mp: 129.4-130.5 °C. ¹H NMR (CDCl₃, 500 MHz): δ 8.20 (s, 1H), 7.97 (d, *J* = 7.5 Hz, 1H), 4.04-3.97 (m, 1H), 3.37-3.31 (m, 1H), 2.04-2.01 (m, 2H),

1.81-1.77 (m, 2H), 1.69-1.65 (m, 1H), 1.49-1.41 (m, 2H), 1.39-1.36 (m, 2H), 1.34 (s, 3H), 1.33 (s, 3H), 1.29-1.24 (m, 1H). MS (ESI), m/z: 282.16 [M+H]⁺.

N-(adamantan-1-yl)-6-chloro-5-isopropylpyridazine-3-carboxamide (20e)

White solid. Yield: 68.6%. Mp: 97.5-98.1 °C. ¹H NMR (CDCl₃, 500 MHz): δ 8.18 (s, 1H), 7.88 (s, 1H), 3.35-3.29 (m, 1H), 2.16 (s, 9H), 1.77-1.69 (m, 6H), 1.32 (s, 3H), 1.31 (s, 3H). MS (ESI), m/z: 334.19 [M+H]⁺.

N-(adamantan-2-yl)-6-chloro-5-isopropylpyridazine-3-carboxamide (20f)

White solid. Yield: 75.0%. Mp: 132.6-134 °C. ¹H NMR (CDCl₃, 500 MHz): δ 8.48 (d, *J* = 7.5 Hz, 1H), 8.21 (s, 1H), 4.29-4.27 (m, 1H), 3.37-3.32 (m, 1H), 2.07 (s, 2H), 1.97 (d, *J* = 13.5 Hz, 2H), 1.92 (s, 6H), 1.79 (s, 2H), 1.70 (d, *J* = 12.5 Hz, 2H), 1.34 (s, 3H), 1.33 (s, 3H). MS (ESI), m/z: 334.20 [M+H]⁺.

5.1.12. General procedures for the preparation of pyridazine-3-carboxamide derivatives

21-44 and 46-52

Aliphatic amine (0.18 mmol) and *N,N*-diisopropylethylamine (61 μL) were added into a solution of intermediate compound **14** or **20** (0.12 mmol) in 1,4-dioxane (2 mL), and the reaction was heated under reflux overnight. After cooling to room temperature, the mixture was poured into water and extracted with ethyl acetate. The organic layer was washed with saturated NaCl aqueous solution, dried over anhydrous MgSO₄, and evaporated *in vacuo*. The residue was purified by flash chromatography on silica gel (200-300 mesh, hexane: ethyl acetate = 5:1 to 1:1) to obtain the compounds **21-44** and **46-52**.

N-cyclohexyl-6-morpholinopyridazine-3-carboxamide (21)

White solid. Yield: 89.7%. Mp: 146.4-147.0 °C. ¹H NMR (CDCl₃, 500 MHz): δ 8.04 (d, *J*

= 9.5 Hz, 1H), 7.85 (d, $J = 7.5$ Hz, 1H), 6.96 (d, $J = 9.5$ Hz, 1H), 4.00-3.94 (m, 1H), 3.86 (t, $J = 4.5$ Hz, 4H), 3.72 (t, $J = 5.0$ Hz, 4H), 2.02-1.99 (m, 2H), 1.79-1.75 (m, 2H), 1.65-1.62 (m, 1H), 1.47-1.39 (m, 2H), 1.34-1.22 (m, 3H). ^{13}C NMR (CDCl_3 , 125 MHz): δ 162.16, 160.37, 145.37, 126.94, 112.10, 66.44, 48.16, 45.01, 33.09, 25.55, 24.79. MS (ESI), m/z : 291.18 $[\text{M}+\text{H}]^+$.

N-(adamantan-1-yl)-6-morpholinopyridazine-3-carboxamide (22)

White solid. Yield: 92.5%. Mp: 191.6-192.0 °C. ^1H NMR (CDCl_3 , 500 MHz): δ 8.02 (d, $J = 9.5$ Hz, 1H), 7.77 (s, 1H), 6.96 (d, $J = 9.5$ Hz, 1H), 3.86 (t, $J = 4.5$ Hz, 4H), 3.72 (t, $J = 5.0$ Hz, 4H), 2.14 (s, 9H), 1.76-1.70 (m, 6H). ^{13}C NMR (CDCl_3 , 125 MHz): δ 162.00, 160.33, 146.01, 126.60, 112.22, 66.43, 51.82, 45.08, 41.65, 36.39, 29.49. MS (ESI), m/z : 343.23 $[\text{M}+\text{H}]^+$.

N-(adamantan-2-yl)-6-morpholinopyridazine-3-carboxamide (23)

White solid. Yield: 85.2%. Mp: 219.4-219.8 °C. ^1H NMR (CDCl_3 , 500 MHz): δ 8.34 (d, $J = 8.0$ Hz, 1H), 8.05 (d, $J = 9.5$ Hz, 1H), 6.97 (d, $J = 9.5$ Hz, 1H), 4.27-4.25 (m, $J = 8.5$ Hz, 1H), 3.86 (t, $J = 4.5$ Hz, 4H), 3.73 (t, $J = 5.0$ Hz, 4H), 2.05 (s, 2H), 1.99 (d, $J = 13.0$ Hz, 2H), 1.90-1.88 (m, 6H), 1.77 (s, 2H), 1.67 (d, $J = 13.0$ Hz, 2H). ^{13}C NMR (CDCl_3 , 125 MHz): δ 162.20, 160.42, 145.62, 126.95, 112.13, 66.44, 53.40, 45.09, 37.59, 37.19, 32.16, 31.90, 27.28, 27.21. MS (ESI), m/z : 343.24 $[\text{M}+\text{H}]^+$.

N-cyclohexyl-4-isopropyl-6-morpholinopyridazine-3-carboxamide (24)

White solid. Yield: 35.4%. Mp: 109.4-110.3 °C. ^1H NMR (CDCl_3 , 500 MHz): δ 7.89 (d, $J = 8.0$ Hz, 1H), 6.80 (s, 1H), 4.34-4.29 (m, 1H), 3.94-3.90 (m, 1H), 3.86 (t, $J = 4.5$ Hz, 4H), 3.70 (t, $J = 5.0$ Hz, 4H), 2.02-1.99 (m, 2H), 1.78-1.71 (m, 2H), 1.66-1.62 (m, 1H), 1.45-1.37

(m, 3H), 1.31-1.28 (m, 2H), 1.26 (s, 3H), 1.24 (s, 3H). ^{13}C NMR (CDCl_3 , 125 MHz): δ 163.95, 160.61, 151.34, 144.01, 108.92, 66.49, 48.21, 45.03, 33.09, 27.77, 25.61, 24.95, 22.86. MS (ESI), m/z : 333.23 $[\text{M}+\text{H}]^+$.

N-(adamantan-1-yl)-4-isopropyl-6-morpholinopyridazine-3-carboxamide (25)

White solid. Yield: 26.0%. Mp: 156.6-158.0 °C. ^1H NMR (CDCl_3 , 500 MHz): δ 7.74 (s, 1H), 6.79 (s, 1H), 4.31-4.25 (m, 1H), 3.86 (t, $J = 5$ Hz, 4H), 3.69 (t, $J = 5.0$ Hz, 4H), 2.14-2.11 (m, 9H), 1.75-1.69 (m, 6H), 1.25 (s, 3H), 1.23 (s, 3H). ^{13}C NMR (CDCl_3 , 125 MHz): δ 164.09, 160.59, 151.14, 144.87, 109.07, 66.49, 51.84, 45.10, 41.58, 36.46, 29.53, 27.72, 22.86. MS (ESI), m/z : 385.27 $[\text{M}+\text{H}]^+$.

N-(adamantan-2-yl)-4-isopropyl-6-morpholinopyridazine-3-carboxamide (26)

White solid. Yield: 29.7%. Mp: 180.6-181.7 °C. ^1H NMR (CDCl_3 , 500 MHz): δ 8.36 (d, $J = 8.0$ Hz, 1H), 6.81 (s, 1H), 4.34-4.29 (m, 1H), 4.22-4.21 (m, 1H), 3.87 (t, $J = 4.5$ Hz, 4H), 3.71 (t, $J = 5.0$ Hz, 4H), 2.05 (s, 2H), 1.98 (d, $J = 13.0$ Hz, 2H), 1.89-1.86 (m, 6H), 1.77 (s, 2H), 1.66 (d, $J = 13.0$ Hz, 2H), 1.26 (s, 3H), 1.25 (s, 3H). ^{13}C NMR (CDCl_3 , 125 MHz): δ 164.06, 160.69, 151.35, 144.31, 108.96, 66.50, 53.44, 45.10, 37.62, 37.25, 32.08, 32.00, 27.81, 27.31, 27.28, 22.88. MS (ESI), m/z : 385.26 $[\text{M}+\text{H}]^+$.

N-cyclohexyl-5-isopropyl-6-morpholinopyridazine-3-carboxamide (27)

White solid. Yield: 44.1%. Mp: 186.3-186.7 °C. ^1H NMR (CDCl_3 , 500 MHz): δ 8.09 (s, 1H), 8.00 (d, $J = 8.0$ Hz, 1H), 4.02-3.96 (m, 1H), 3.91 (t, $J = 4.5$ Hz, 4H), 3.35 (t, $J = 4.5$ Hz, 4H), 3.18-3.13 (m, 1H), 2.02-1.99 (m, 2H), 1.79-1.75 (m, 2H), 1.67-1.63 (m, 1H), 1.49-1.40 (m, 3H), 1.35-1.32 (m, 1H), 1.30 (s, 3H), 1.29 (s, 3H), 1.27-1.23 (m, 1H). ^{13}C NMR (CDCl_3 , 125 MHz): δ 163.75, 162.01, 149.45, 142.94, 124.60, 66.80, 51.43, 48.23, 33.01, 27.52,

25.53, 24.74, 23.12. MS (ESI), m/z: 333.23 [M+H]⁺.

N-(adamantan-1-yl)-5-isopropyl-6-morpholinopyridazine-3-carboxamide (28)

White solid. Yield: 47.4%. Mp: 149.7-150.0 °C. ¹H NMR (CDCl₃, 500 MHz): δ 8.08 (s, 1H), 7.91 (s, 1H), 3.91 (t, *J* = 4.5 Hz, 4H), 3.34 (t, *J* = 4.5 Hz, 4H), 3.17-3.12 (m, 1H), 2.15 (s, 9H), 1.77-1.71 (m, 6H), 1.29 (s, 3H), 1.28 (s, 3H). ¹³C NMR (CDCl₃, 125 MHz): δ 163.66, 161.86, 150.02, 142.95, 124.26, 66.80, 51.96, 51.44, 41.55, 36.36, 29.45, 27.49, 23.08. MS (ESI), m/z: 385.25 [M+H]⁺.

N-(adamantan-2-yl)-5-isopropyl-6-morpholinopyridazine-3-carboxamide (29)

White solid. Yield: 58.2%. Mp: 232.2-232.6 °C. ¹H NMR (CDCl₃, 500 MHz): δ 8.49 (d, *J* = 8.5 Hz, 1H), 8.11 (s, 1H), 4.29-4.27 (m, 1H), 3.92 (t, *J* = 4.5 Hz, 4H), 3.35 (t, *J* = 5.0 Hz, 4H), 3.19-3.14 (m, 1H), 2.05 (s, 2H), 2.00 (d, *J* = 13.5 Hz, 2H), 1.91-1.88 (m, 6H), 1.78 (s, 2H), 1.68 (d, *J* = 12.0 Hz, 2H), 1.31 (s, 3H), 1.29 (s, 3H). ¹³C NMR (CDCl₃, 125 MHz): δ 163.83, 162.07, 149.74, 142.97, 124.60, 66.82, 53.53, 51.50, 37.58, 37.18, 32.15, 31.89, 27.54, 27.28, 27.20, 23.07. MS (ESI), m/z: 385.26 [M+H]⁺.

N-cyclohexyl-6-(cyclopentylamino)-4-isopropylpyridazine-3-carboxamide (30)

White solid. Yield: 10.0%. Mp: 172.1-173.1 °C. ¹H NMR (CDCl₃, 500 MHz): δ 7.89 (d, *J* = 8.0 Hz, 1H), 6.55 (s, 1H), 4.89 (s, 1H), 4.30-4.23 (m, 2H), 3.94-3.86 (m, 1H), 2.17-2.10 (m, 2H), 2.01-1.98 (m, 2H), 1.79-1.74 (m, 4H), 1.70-1.67 (m, 1H), 1.65-1.62 (m, 2H), 1.56-1.49 (m, 2H), 1.45-1.34 (m, 3H), 1.30-1.26 (m, 2H), 1.23(s, 3H), 1.22 (s, 3H). ¹³C NMR (CDCl₃, 125 MHz): δ 164.20, 159.79, 151.21, 143.77, 110.00, 53.35, 48.17, 33.40, 33.13, 27.54, 25.65, 24.99, 23.81, 22.78. MS (ESI), m/z: 331.27 [M+H]⁺.

6-(butylamino)-N-cyclohexyl-4-isopropylpyridazine-3-carboxamide (31)

Yellow solid. Yield: 16.2%. Mp: 109.5-110.7 °C. ^1H NMR (CDCl_3 , 500 MHz): δ 7.89 (d, J = 8.0 Hz, 1H), 6.54 (s, 1H), 4.81 (s, 1H), 4.30-4.25 (m, 1H), 3.94-3.86 (m, 1H), 3.48-3.44 (q, 2H), 2.01-1.98 (m, 2H), 1.78-1.74 (m, 2H), 1.70-1.64 (m, 2H), 1.63-1.61 (m, 1H), 1.49-1.45 (m, 2H), 1.43-1.33 (m, 3H), 1.31-1.26 (m, 2H), 1.23(s, 3H), 1.22 (s, 3H), 0.98 (t, J = 7.5 Hz, 3H). ^{13}C NMR (CDCl_3 , 125 MHz): δ 164.18, 160.05, 151.28, 143.87, 109.81, 48.16, 41.70, 33.12, 31.50, 27.57, 25.64, 24.98, 22.80, 20.15, 13.81. MS (ESI), m/z : 319.25 $[\text{M}+\text{H}]^+$.

N-cyclohexyl-6-((2-hydroxyethyl)amino)-4-isopropylpyridazine-3-carboxamide (32)

White solid. Yield: 11.6%. Mp: 169.2-171.2 °C. ^1H NMR (CDCl_3 , 500 MHz): δ 7.78 (d, J = 7.5 Hz, 1H), 6.63 (s, 1H), 5.46 (s, 1H), 4.26-4.20 (m, 1H), 3.92 (t, J = 5.0 Hz, 2H), 3.94-3.87 (m, 1H), 3.71-3.68 (q, 2H), 2.02-1.98 (m, 2H), 1.78-1.74 (m, 2H), 1.65-1.61 (m, 1H), 1.48-1.36 (m, 3H), 1.31-1.26 (m, 2H), 1.23 (s, 3H), 1.21 (s, 3H). ^{13}C NMR (CDCl_3 , 125 MHz): δ 164.00, 160.00, 151.48, 144.57, 111.26, 62.12, 48.23, 44.48, 33.07, 27.60, 25.63, 24.94, 27.75. MS (ESI), m/z : 307.23 $[\text{M}+\text{H}]^+$.

N-(adamantan-1-yl)-6-(cyclopentylamino)-4-isopropylpyridazine-3-carboxamide (33)

White solid. Yield: 12.4%. Mp: 229.6-230.6 °C. ^1H NMR (CDCl_3 , 500 MHz): δ 7.73 (s, 1H), 6.54 (s, 1H), 4.87 (s, 1H), 4.27-4.21 (m, 2H), 2.15-2.11 (m, 11H), 1.78-1.68 (m, 10H), 1.55-1.50 (m, 2H), 1.22 (s, 3H), 1.21 (s, 3H). ^{13}C NMR (CDCl_3 , 125 MHz): δ 164.33, 159.69, 151.04, 144.50, 110.23, 53.31, 51.73, 41.58, 36.48, 33.40, 29.53, 27.51, 23.80, 22.81. MS (ESI), m/z : 383.30 $[\text{M}+\text{H}]^+$.

N-(adamantan-1-yl)-6-(butylamino)-4-isopropylpyridazine-3-carboxamide (34)

White solid. Yield: 11.2%. Mp: 77.2-73.0 °C. ^1H NMR (CDCl_3 , 500 MHz): δ 7.74 (s, 1H), 6.53 (s, 1H), 4.79 (s, 1H), 4.27-4.21 (m, 1H), 3.47-3.43 (q, 2H), 2.13-2.11 (m, 9H), 1.75-1.69

(m, 6H), 1.68-1.63 (m, 2H), 1.49-1.41 (m, 2H), 1.22 (s, 3H), 1.21 (s, 3H), 0.97 (t, $J = 7.5$ Hz, 3H). ^{13}C NMR (CDCl_3 , 125 MHz): δ 164.32, 159.99, 151.09, 144.72, 109.91, 51.72, 41.70, 41.60, 36.49, 31.53, 29.55, 27.50, 22.79, 20.13, 13.77. MS (ESI), m/z : 371.29 $[\text{M}+\text{H}]^+$.

N-(adamantan-1-yl)-6-((2-hydroxyethyl)amino)-4-isopropylpyridazine-3-carboxamide (35)

Yellow solid. Yield: 12.6%. Mp: 82.4-83.2 °C. ^1H NMR (CDCl_3 , 500 MHz): δ 7.58 (s, 1H), 6.61 (s, 1H), 5.48 (s, 1H), 4.22-4.17 (m, 1H), 3.92-3.90 (t, $J = 5.0$ Hz, 2H), 3.70-3.67 (m, 2H), 2.13-2.11 (m, 9H), 1.75-1.68 (m, 6H), 1.22 (s, 3H), 1.21 (s, 3H). ^{13}C NMR (CDCl_3 , 125 MHz): δ 164.17, 160.11, 151.31, 145.31, 111.14, 61.94, 51.88, 44.59, 41.54, 36.45, 29.52, 27.59, 27.73. MS (ESI), m/z : 359.27 $[\text{M}+\text{H}]^+$.

N-(adamantan-2-yl)-6-(cyclopentylamino)-4-isopropylpyridazine-3-carboxamide (36)

Yellow solid. Yield: 10.2%. Mp: 138.8-139.2 °C. ^1H NMR (CDCl_3 , 500 MHz): δ 8.36 (d, $J = 8.0$ Hz, 1H), 6.55 (s, 1H), 4.81 (d, $J = 6.0$ Hz, 1H), 4.31-4.24 (m, 2H), 4.21-4.19 (m, 1H), 2.17-2.11 (m, 2H), 2.04 (s, 2H), 1.98 (d, $J = 13.0$ Hz, 2H), 1.89-1.86 (m, 6H), 1.79-1.76 (m, 4H), 1.70-1.68 (m, 2H), 1.65 (d, $J = 13.0$ Hz, 2H), 1.54-1.50 (m, 2H), 1.23 (s, 3H), 1.22 (s, 3H). ^{13}C NMR (CDCl_3 , 125 MHz): δ 164.28, 159.76, 151.25, 143.88, 110.23, 53.34, 53.32, 37.66, 37.26, 33.38, 32.11, 32.00, 27.60, 27.33, 27.29, 23.81, 22.80. MS (ESI), m/z : 383.28 $[\text{M}+\text{H}]^+$.

N-(adamantan-2-yl)-6-(butylamino)-4-isopropylpyridazine-3-carboxamide (37)

White solid. Yield: 40.5%. Mp: 116.2-117.7 °C. ^1H NMR (CDCl_3 , 500 MHz): δ 8.38 (d, $J = 8.0$ Hz, 1H), 6.56 (s, 1H), 4.89 (s, 1H), 4.30-4.24 (m, 1H), 4.20 (d, $J = 8.5$ Hz, 1H), 3.50-3.46 (m, 2H), 2.03 (s, 2H), 1.97 (d, $J = 13.0$ Hz, 2H), 1.88-1.86 (m, 6H), 1.76 (s, 2H), 1.70-1.63 (m, 4H), 1.49-1.42 (m, 2H), 1.23 (s, 3H), 1.22 (s, 3H), 0.97 (t, $J = 7.5$ Hz, 3H). ^{13}C NMR

(CDCl₃, 125 MHz): δ 164.27, 160.06, 151.30, 144.10, 109.91, 53.35, 41.71, 37.64, 37.27, 32.10, 31.98, 31.51, 27.61, 27.32, 27.28, 22.82, 20.14, 13.81. MS (ESI), m/z: 371.30 [M+H]⁺.

N-(adamantan-2-yl)-6-((2-hydroxyethyl)amino)-4-isopropylpyridazine-3-carboxamide (38)

White solid. Yield: 28.5%. Mp: 79.4-82.0 °C. ¹H NMR (CDCl₃, 500 MHz): δ 8.19 (s, 1H), 6.64 (s, 1H), 5.90 (s, 1H), 4.23-4.19 (m, 2H), 3.93-3.91 (m, 2H), 3.67-3.65 (m, 2H), 2.03 (s, 2H), 1.97(d, *J* = 13.0 Hz, 2H), 1.88-1.86 (m, 6H), 1.76 (s, 2H), 1.66 (d, *J* = 13.0 Hz, 2H), 1.23 (s, 3H), 1.21 (s, 3H). ¹³C NMR (CDCl₃, 125 MHz): δ 164.14, 160.18, 151.52, 144.61, 111.12, 61.88, 53.46, 44.54, 37.60, 37.24, 32.06, 31.96, 27.69, 27.29, 27.25, 22.78. MS (ESI), m/z: 359.28 [M+H]⁺.

N-(adamantan-2-yl)-4-isopropyl-6-(piperidin-1-yl)pyridazine-3-carboxamide (39)

White solid. Yield: 55.7%. Mp: 175.4-176.9 °C. ¹H NMR (CDCl₃, 500 MHz): δ 8.39 (d, *J* = 8.0 Hz, 1H), 6.80 (s, 1H), 4.32-4.27 (m, 1H), 4.22-4.20 (m, 1H), 3.72 (t, *J* = 5.5 Hz, 4H), 2.04 (s, 2H), 1.99 (d, *J* = 13.0 Hz, 2H), 1.89-1.85 (m, 6H), 1.76 (s, 2H), 1.72-1.66 (m, 8H), 1.25 (s, 3H), 1.24 (s, 3H). ¹³C NMR (CDCl₃, 125 MHz): δ 164.33, 160.47, 150.96, 143.01, 108.77, 53.34, 46.01, 37.65, 37.27, 32.10, 31.99, 27.77, 27.31, 27.29, 25.46, 24.55, 22.91. MS (ESI), m/z: 383.28 [M+H]⁺.

N-(adamantan-2-yl)-4-isopropyl-6-(4-methylpiperazin-1-yl)pyridazine-3-carboxamide (40)

Yellow solid. Yield: 28.9%. Mp: 154.8-155.8 °C. ¹H NMR (CDCl₃, 500 MHz): δ 8.38 (d, *J* = 8.0 Hz, 1H), 6.82 (s, 1H), 4.33-4.28 (m, 1H), 4.22-4.20 (m, 1H), 3.77 (t, *J* = 5.0 Hz, 4H), 2.57 (t, *J* = 5.0 Hz, 4H), 2.37 (s, 3H), 2.04 (s, 2H), 1.98 (d, *J* = 12.5 Hz, 2H), 1.89-1.86 (m, 6H), 1.76 (s, 2H), 1.65 (d, *J* = 12.5 Hz, 2H), 1.26 (s, 3H), 1.24 (s, 3H). ¹³C NMR (CDCl₃, 125 MHz): δ 164.15, 160.52, 151.19, 143.79, 108.99, 54.59, 53.38, 46.15, 44.70, 37.62, 37.25,

32.08, 31.98, 27.80, 27.30, 27.27, 22.89. MS (ESI), m/z: 398.31 [M+H]⁺.

N-(adamantan-2-yl)-6-(cyclohexylamino)-4-isopropylpyridazine-3-carboxamide (41)

White solid. Yield: 62.8%. Mp: 189.4-190.7 °C. ¹H NMR (CDCl₃, 500 MHz): δ 8.33 (d, *J* = 8.0 Hz, 1H), 6.52 (s, 1H), 4.81-4.80 (m, 1H), 4.27-4.22 (m, 1H), 4.20-4.18 (m, 1H), 3.93-3.92 (m, 1H), 2.11-2.08 (m, 2H), 2.02 (s, 2H), 1.97 (d, *J* = 13.0 Hz, 2H), 1.87-1.84 (m, 6H), 1.79-1.76 (m, 2H), 1.75 (s, 2H), 1.68-1.67 (m, 1H), 1.64 (d, *J* = 13.0 Hz, 2H), 1.48-1.39 (m, 2H), 1.29-1.24 (m, 3H), 1.21 (s, 3H), 1.20 (s, 3H). ¹³C NMR (CDCl₃, 125 MHz): δ 164.33, 159.31, 151.14, 143.98, 110.39, 53.39, 49.95, 37.64, 37.27, 33.20, 32.09, 31.98, 27.56, 27.32, 27.30, 25.65, 24.79, 22.79. MS (ESI), m/z: 397.30 [M+H]⁺.

N-(adamantan-2-yl)-6-(cyclopropylamino)-4-isopropylpyridazine-3-carboxamide (42)

White solid. Yield: 81.6%. Mp: 224.5-225.9 °C. ¹H NMR (CDCl₃, 500 MHz): δ 8.39 (d, *J* = 8.0 Hz, 1H), 6.89 (s, 1H), 6.00-5.96 (m, 1H), 4.33-4.28 (m, 1H), 4.20 (d, *J* = 8.0 Hz, 1H), 2.66-2.62 (m, 1H), 2.04 (s, 2H), 1.97 (d, *J* = 13.0 Hz, 2H), 1.90-1.86 (m, 6H), 1.76 (s, 2H), 1.65 (d, *J* = 12.5 Hz, 2H), 1.26 (s, 3H), 1.25 (s, 3H), 0.91-0.87 (m, 2H), 0.66-0.63 (m, 2H). ¹³C NMR (CDCl₃, 125 MHz): δ 164.27, 161.87, 151.77, 144.51, 108.76, 53.35, 37.65, 37.27, 32.12, 32.01, 27.70, 27.34, 27.30, 23.76, 22.84, 7.60. MS (ESI), m/z: 355.27 [M+H]⁺.

N-(adamantan-2-yl)-6-((cyclopropylmethyl)amino)-4-isopropylpyridazine-3-carboxamide (43)

White solid. Yield: 31.3%. Mp: 138.3-139.5 °C. ¹H NMR (CDCl₃, 500 MHz): δ 8.38 (d, *J* = 8.0 Hz, 1H), 8.59 (s, 1H), 4.97 (s, 1H), 4.30-4.25 (m, 1H), 4.20 (d, *J* = 8.5 Hz, 1H), 3.36-3.34 (m, 2H), 2.03 (s, 2H), 1.98 (d, *J* = 13.0 Hz, 2H), 1.90-1.86 (m, 6H), 1.76 (s, 2H), 1.65 (d, *J* = 12.5 Hz, 2H), 1.24 (s, 3H), 1.22 (s, 3H), 1.18-1.12 (m, 1H), 0.62-0.58 (m, 2H),

0.32-0.29 (m, 2H). ^{13}C NMR (CDCl_3 , 125 MHz): δ 164.24, 159.82, 151.32, 144.19, 110.21, 53.34, 46.96, 37.64, 37.26, 32.10, 31.99, 27.61, 27.31, 27.28, 22.83, 10.73, 3.59. MS (ESI), m/z : 369.29 $[\text{M}+\text{H}]^+$.

N-(adamantan-2-yl)-4-isopropyl-6-((3-methylbutan-2-yl)amino)pyridazine-3-carboxamide (44)

White solid. Yield: 33.0%. Mp: 167.2-168.7 °C. ^1H NMR (CDCl_3 , 500 MHz): δ 8.36 (d, J = 8.0 Hz, 1H), 6.54 (s, 1H), 4.72 (s, 1H), 4.29-4.24 (m, 1H), 4.20 (d, J = 8.5 Hz, 1H), 4.04-4.01 (m, 1H), 2.03 (s, 2H), 1.98 (d, J = 13.5 Hz, 2H), 1.90-1.86 (m, 7H), 1.76 (s, 2H), 1.65 (d, J = 12.5 Hz, 2H), 1.24-1.21 (m, 9H), 1.01 (d, J = 7.0 Hz, 3H), 0.97 (d, J = 7.0 Hz, 3H). ^{13}C NMR (CDCl_3 , 125 MHz): δ 164.26, 159.72, 151.31, 143.95, 110.25, 53.36, 52.01, 37.65, 37.27, 32.93, 32.10, 31.99, 27.61, 27.32, 27.30, 22.83, 22.80, 18.85, 18.13, 17.23. MS (ESI), m/z : 385.30 $[\text{M}+\text{H}]^+$.

N-(adamantan-2-yl)-5-isopropyl-6-(piperidin-1-yl)pyridazine-3-carboxamide (46)

White solid. Yield: 92.6%. Mp: 227.7-228.5 °C. ^1H NMR (CDCl_3 , 500 MHz): δ 8.50 (d, J = 8.0 Hz, 1H), 8.04 (s, 1H), 4.27-4.25 (m, 1H), 3.26 (t, J = 5.0 Hz, 4H), 3.16-3.11 (m, 1H), 2.03 (s, 2H), 1.99 (d, J = 13.5 Hz, 2H), 1.93-1.87 (m, 6H), 1.76-1.74 (m, 6H), 1.68-1.65 (m, 4H), 1.28 (s, 3H), 1.27 (s, 3H). ^{13}C NMR (CDCl_3 , 125 MHz): δ 164.92, 162.34, 149.10, 142.98, 124.14, 53.42, 52.41, 37.60, 37.19, 32.16, 31.87, 27.66, 27.29, 27.22, 26.02, 24.28, 23.06. MS (ESI), m/z : 383.29 $[\text{M}+\text{H}]^+$.

N-(adamantan-2-yl)-6-(cyclohexylamino)-5-isopropylpyridazine-3-carboxamide (47)

White solid. Yield: 34.2%. Mp: 184.7-185.9 °C. ^1H NMR (CDCl_3 , 500 MHz): δ 8.35 (d, J = 8.0 Hz, 1H), 7.85 (s, 1H), 4.49 (d, J = 7.5 Hz, 1H), 4.34-4.28 (m, 1H), 4.25-4.23 (m, 1H),

2.70-2.64 (m, 1H), 2.18-2.15 (m, 2H), 2.03 (s, 2H), 2.00 (d, $J = 13.0$ Hz, 2H), 1.92-1.86 (m, 6H), 1.79-1.78 (m, 2H), 1.76 (s, 2H), 1.70-1.67 (m, 1H), 1.64 (d, $J = 12.5$ Hz, 2H), 1.53-1.45 (m, 2H), 1.29 (s, 3H), 1.28 (s, 3H), 1.30-1.24 (m, 3H). ^{13}C NMR (CDCl_3 , 125 MHz): δ 163.02, 156.92, 145.56, 132.85, 121.48, 53.38, 49.92, 37.62, 37.21, 33.34, 32.13, 31.86, 27.29, 27.24, 26.97, 25.79, 24.94, 20.70. MS (ESI), m/z : 397.31 $[\text{M}+\text{H}]^+$.

N-(adamantan-2-yl)-6-(cyclopentylamino)-5-isopropylpyridazine-3-carboxamide (48)

White solid. Yield: 53.9%. Mp: 186.1-186.9 °C. ^1H NMR (CDCl_3 , 500 MHz): δ 8.38 (d, $J = 8.0$ Hz, 1H), 7.85 (s, 1H), 4.66-4.62 (m, 1H), 4.61-4.58 (m, 1H), 4.25-4.24 (d, $J = 8.0$ Hz, 1H), 2.70-2.64 (m, 1H), 2.25-2.19 (m, 2H), 2.03 (s, 2H), 1.99 (d, $J = 13.0$ Hz, 2H), 1.92-1.86 (m, 6H), 1.78-1.69 (m, 6H), 1.64 (d, $J = 12.5$ Hz, 2H), 1.55-1.48 (m, 2H), 1.29 (s, 3H), 1.27 (s, 3H). ^{13}C NMR (CDCl_3 , 125 MHz): δ 163.00, 157.29, 145.62, 133.03, 121.34, 53.46, 53.34, 37.63, 37.21, 33.56, 32.15, 31.86, 27.29, 27.24, 26.99, 23.81, 20.73. MS (ESI), m/z : 383.28 $[\text{M}+\text{H}]^+$.

N-(adamantan-2-yl)-6-((cyclopropylmethyl)amino)-5-isopropylpyridazine-3-carboxamide (49)

White solid. Yield: 27.4%. Mp: 202.5-203 °C. ^1H NMR (CDCl_3 , 500 MHz): δ 8.41 (d, $J = 8.0$ Hz, 1H), 7.88 (s, 1H), 4.78-4.76 (m, 1H), 4.25 (d, $J = 8.5$ Hz, 1H), 3.53-3.51 (m, 2H), 2.78-2.73 (m, 1H), 2.04 (s, 2H), 2.00 (d, $J = 13.0$ Hz, 2H), 1.93-1.87 (m, 6H), 1.77 (s, 2H), 1.65 (d, $J = 14.0$ Hz, 2H), 1.33 (s, 3H), 1.31 (s, 3H), 1.24-1.18 (m, 1H), 0.63-0.59 (m, 2H), 0.34-0.31 (m, 2H). ^{13}C NMR (CDCl_3 , 125 MHz): δ 162.92, 157.53, 145.92, 133.12, 121.40, 53.33, 47.37, 37.65, 37.23, 32.19, 31.89, 27.32, 27.26, 27.04, 20.77, 10.76, 3.56. MS (ESI), m/z : 369.27 $[\text{M}+\text{H}]^+$.

N-(adamantan-2-yl)-6-(butylamino)-5-isopropylpyridazine-3-carboxamide (50)

White solid. Yield: 45.8%. Mp: 78.6-79.9 °C. ¹H NMR (CDCl₃, 500 MHz): δ 8.39 (d, *J* = 8.5 Hz, 1H), 7.86 (s, 1H), 4.66-4.64 (m, 1H), 4.24 (d, *J* = 8.5 Hz, 1H), 3.70-3.66 (m, 2H), 2.72-2.66 (m, 1H), 2.03 (s, 2H), 1.99 (d, *J* = 13.5 Hz, 2H), 1.92-1.86 (m, 6H), 1.76 (s, 2H), 1.74-1.68 (m, 2H), 1.64 (d, *J* = 12.5 Hz, 2H), 1.50-1.42 (m, 2H), 1.30 (s, 3H), 1.28 (s, 3H). ¹³C NMR (CDCl₃, 125 MHz): δ 162.95, 157.55, 145.71, 133.10, 121.34, 53.30, 42.02, 37.61, 37.19, 32.15, 31.86, 31.53, 27.28, 27.22, 27.01, 20.77, 20.33, 13.89. MS (ESI), *m/z*: 371.28 [M+H]⁺.

N-(adamantan-2-yl)-5-isopropyl-6-(pentan-3-ylamino)pyridazine-3-carboxamide (51)

Yellow oil. Yield: 18.7%. ¹H NMR (CDCl₃, 500 MHz): δ 8.37 (d, *J* = 8.0 Hz, 1H), 7.86 (s, 1H), 4.46-4.42 (m, 1H), 4.35 (d, *J* = 8.5 Hz, 1H), 4.25 (d, *J* = 8.0 Hz, 1H), 2.72-2.66 (m, 1H), 2.03 (s, 2H), 2.00 (d, *J* = 13.0 Hz, 2H), 1.93-1.86 (m, 6H), 1.78-1.73 (m, 4H), 1.65 (d, *J* = 13.0 Hz, 2H), 1.62-1.56 (m, 2H), 1.32 (s, 3H), 1.30 (s, 3H), 0.97 (t, *J* = 7.5 Hz, 6H). ¹³C NMR (CDCl₃, 125 MHz): δ 163.00, 157.69, 145.51, 132.70, 121.46, 53.43, 53.36, 37.64, 37.23, 32.17, 31.88, 27.30, 27.26, 27.05, 26.94, 20.75, 10.13. MS (ESI), *m/z*: 385.30 [M+H]⁺.

N-(adamantan-2-yl)-6-((2-hydroxyethyl)amino)-5-isopropylpyridazine-3-carboxamide (52)

White solid. Yield: 93.9%. Mp: 73.1-75.1 °C. ¹H NMR (CDCl₃, 500 MHz): δ 8.35 (d, *J* = 8.0 Hz, 1H), 7.88 (s, 1H), 5.27-5.25 (m, 1H), 4.23 (d, *J* = 8.0 Hz, 1H), 3.95 (t, *J* = 4.5 Hz, 2H), 3.87-3.84 (q, 2H), 2.78-2.72 (m, 1H), 2.03 (s, 2H), 1.98 (d, *J* = 13.0 Hz, 2H), 1.90-1.87 (m, 6H), 1.76 (s, 2H), 1.66 (d, *J* = 12.5 Hz, 2H), 1.30 (s, 3H), 1.28 (s, 3H). ¹³C NMR (CDCl₃, 125 MHz): δ 162.78, 157.97, 146.12, 133.99, 121.71, 62.23, 53.38, 44.74, 37.58, 37.18, 32.13, 31.88, 27.26, 27.19, 27.08, 20.78. MS (ESI), *m/z*: 359.27 [M+H]⁺.

5.1.13. General procedures for the preparation of pyridazine-3-carboxamide derivatives 45 and 53

Aromatic amines (0.18 mmol) and *N,N*-diisopropylethylamine (61 μ L) were added into a solution of intermediate compound **20c** or **20f** (0.12 mmol) in acetonitrile (2 mL), and the reaction was heated under reflux overnight. Then the mixture was heated at 160 °C until the reaction was completed (TLC monitoring). After cooling to room temperature, the reaction mixture was poured into water and extracted with ethyl acetate. The organic layer was washed with saturated NaCl aqueous solution, dried over anhydrous MgSO_4 , and evaporated *in vacuo*. The residue was purified by flash chromatography on silica gel (200-300 mesh, hexane: ethyl acetate = 5:1 to 4:1) to obtain the compounds **45** and **53**.

***N*-(adamantan-2-yl)-6-((3-chlorophenyl)amino)-4-isopropylpyridazine-3-carboxamide (45)**

White solid. Yield: 19.2%. Mp: 178.2-179.0 °C. ^1H NMR (CDCl_3 , 500 MHz): δ 8.33 (d, J = 8.0 Hz, 1H), 7.92 (s, 1H), 7.52-7.51 (m, 1H), 7.36-7.34 (m, 1H), 7.30 (t, J = 7.5 Hz, 1H), 7.11 (d, J = 8.0 Hz, 1H), 7.08 (s, 1H), 4.33-4.28 (m, 1H), 4.24-4.23 (m, 1H), 2.07 (s, 2H), 1.96 (d, J = 13.5 Hz, 2H), 1.90 (s, 6H), 1.78 (s, 2H), 1.68 (d, J = 12.5 Hz, 2H), 1.25 (s, 3H), 1.23 (s, 3H). ^{13}C NMR (CDCl_3 , 125 MHz): δ 163.80, 158.40, 152.09, 146.05, 140.28, 135.15, 130.47, 123.95, 120.67, 118.67, 111.49, 53.57, 37.59, 37.23, 32.06, 32.04, 27.83, 27.30, 27.24, 22.78. MS (ESI), m/z : 425.21 $[\text{M}+\text{H}]^+$.

***N*-(adamantan-2-yl)-6-((3-chlorophenyl)amino)-5-isopropylpyridazine-3-carboxamide (53)**

White solid. Yield: 11.1%. Mp: 219.1-220.0 °C. ^1H NMR (CDCl_3 , 500 MHz): δ 8.41 (d, J = 8.0 Hz, 1H), 8.05 (s, 1H), 7.75-7.74 (m, 1H), 7.55-7.53 (m, 1H), 7.32 (t, J = 8.0 Hz, 1H), 7.11 (d, J = 8.0 Hz, 1H), 6.53 (s, 1H), 4.28-4.26 (m, 1H), 2.95-2.89 (m, 1H), 2.06 (s, 2H),

2.00 (d, $J = 13.0$ Hz, 2H), 1.91-1.89 (m, 6H), 1.78 (s, 2H), 1.67 (d, $J = 13.0$ Hz, 2H), 1.40 (s, 3H), 1.38(s, 3H). ^{13}C NMR (CDCl_3 , 125 MHz): δ 162.37, 155.95, 147.97, 140.30, 134.78, 134.63, 130.10, 123.81, 122.60, 121.13, 119.19, 53.63, 37.61, 37.21, 32.11, 31.91, 27.37, 27.29, 27.24, 21.07. MS (ESI), m/z : 425.20 $[\text{M}+\text{H}]^+$.

5.2. Biological assays

Chinese hamster ovarian (CHO) cells stably expressing $\text{G}\alpha_{16}$ with either CB1 or CB2 receptor were seeded onto 96-well plates and incubated for 24 h. Cells were loaded with 2 μM fluo-4 AM in Hanks balanced salt solution (HBSS, containing 5.4 mM KCl, 0.3 mM Na_2HPO_4 , 0.4 mM KH_2PO_4 , 4.2 mM NaHCO_3 , 1.3 mM CaCl_2 , 0.5 mM MgCl_2 , 0.6 mM MgSO_4 , 137.0 mM NaCl, 5.6 mM D-glucose and 250 μM sulfinpyrazone, pH 7.4) at 37 °C for 45 min. In the agonist mode, 50 μL HBSS was added to the dye-load cells, and 25 μL of the test compounds with variable concentrations ranging from 10 pM to 100 μM , CP55940 (positive control) or DMSO (negative control) were added with FlexStation. Meanwhile, the intracellular calcium change was recorded at an excitation wavelength of 485 nm and an emission wavelength of 525 nm. In the antagonist mode, the excess dye was removed and 50 μL HBSS containing test compounds, SR141716A (positive control) or DMSO (negative control) was added. After 10 min incubation at room temperature, 25 μL CP55940 was dispensed into the wells using a FlexStation microplate reader, and intracellular calcium change was recorded at an excitation wavelength of 485 nm and an emission wavelength of 525 nm. All experiments were performed in triplicate. EC_{50} and IC_{50} values were analyzed with sigmoidal dose-response curve fitting using GraphPad Prism.

5.3. Docking simulations

The 3D structures of all studied ligands are constructed using the SKETCH molecule of Sybyl-X1.3 software [47]. The geometry optimization of all compounds is carried out by using the Tripos force field with the Gasteiger-Hückel atomic charge, and repeated minimization is performed using Powell conjugated gradient algorithm method with a convergence criterion of 0.001 kcal/(mol·Å). The binding site of CB2 receptor homology model was determined on the basis of our previous published data [53]. Flexible docking simulations were performed to predict the possible binding conformations of each ligand in the active pocket of CB2 receptor using the FlexiDock method of Sybyl-X1.3 [47]. Prior to docking simulations, a binding pocket was elucidated taking into account the area around 5 Å of the ligand in the initial receptor-ligand complex. During the docking process, all the single bonds of the ligand as well as the side chains of residues within the potential binding pocket were regarded as rotatable bonds, and the ligand was allowed to move freely. The H-bonding sites were marked for the suitable atoms of both the CB2 receptor and ligand, and the top 20 scored receptor-ligand complexes were kept for further analysis. For each system, the obtained 20 best scoring complex models have very similar 3D structures with little different energies. Therefore, only one best CB2-ligand complex was selected to analyze the interaction modes of our synthesized ligand with CB2 receptor.

Acknowledgements

This project was supported by grants from the National Natural Science Foundation of

China (30973637, 81425024, 81473135), the Ministry of Science and Technology (2014CB541906), and Zhejiang Technology Office (Qianjiang Talents Project 2010R10048).

Appendix A. Supplementary data

Supplementary data related to this article can be found at <http://www.sciencedirect.com>.

The data include the docking results of the lead compound GW842166X, the activation of synthesized compounds and GW842166X at 10 μ M, superimposition of docking results of compounds **24-26**, and ^1H NMR spectra of compounds **7a** and **7b**.

References

- [1] J.C. Ashton, J.L. Wright, J.M. McPartland, J.D. Tyndall, Cannabinoid CB1 and CB2 receptor ligand specificity and the development of CB2-selective agonists, *Curr. Med. Chem.*, 15 (2008) 1428-1443.
- [2] L.A. Matsuda, S.J. Lolait, M.J. Brownstein, A.C. Young, T.I. Bonner, Structure of a cannabinoid receptor and functional expression of the cloned cDNA, *Nature*, 346 (1990) 561-564.
- [3] S. Munro, K.L. Thomas, M. Abu-Shaar, Molecular characterization of a peripheral receptor for cannabinoids, *Nature*, 365 (1993) 61-65.
- [4] P. Pacher, S. B atkai, G. Kunos, The endocannabinoid system as an emerging target of pharmacotherapy, *Pharmacol. Rev.*, 58 (2006) 389-462.
- [5] M.R. Elphick, M. Egertova, The neurobiology and evolution of cannabinoid signalling, *Philos. Trans. R. Soc. Lond. B Biol. Sci.*, 356 (2001) 381-408.
- [6] R.P. Picone, D.A. Kendall, Minireview: from the bench, toward the clinic: therapeutic opportunities for cannabinoid receptor modulation, *Mol. Endocrinol.*, 29 (2015) 801-813.
- [7] G.A. Thakur, S.P. Nikas, A. Makriyannis, CB1 cannabinoid receptor ligands, *Mini-Rev. Med. Chem.*, 5 (2005) 631-640.
- [8] D. Jones, End of the line for cannabinoid receptor 1 as an anti-obesity target?, *Nat. Rev. Drug Discov.*, 7 (2008) 961-962.
- [9] I. Sv i ensk a, P. Dubov y, A.  ulcov a, Cannabinoid receptors 1 and 2 (CB1 and CB2), their distribution, ligands and functional involvement in nervous system structures-a short review, *Pharmacol. Biochem. Be.*, 90 (2008) 501-511.
- [10] R. Feng, C.A. Milcarek, X.-Q. Xie, Antagonism of cannabinoid receptor 2 pathway suppresses IL-6-induced immunoglobulin IgM secretion, *BMC Pharmacol. Toxicol.*, 15 (2014) 30.
- [11] P. Massi, A. Vaccani, D. Parolaro, Cannabinoids, immune system and cytokine network, *Curr. Pharm. Des.*, 12 (2006) 3135-3146.
- [12] G.A. Cabral, L. Griffin-Thomas, Emerging role of the cannabinoid receptor CB 2 in immune regulation:

- therapeutic prospects for neuroinflammation, *Expert Rev. Mol. Med.*, 11 (2009) e3.
- [13] M. Beltramo, Cannabinoid type 2 receptor as a target for chronic-pain, *Mini-Rev. Med. Chem.*, 9 (2009) 11-25.
- [14] J. Guindon, A. Hohmann, Cannabinoid CB2 receptors: a therapeutic target for the treatment of inflammatory and neuropathic pain, *Br. J. Pharmacol.*, 153 (2008) 319-334.
- [15] M. Karsak, M. Cohen-Solal, J. Freudenberg, A. Ostertag, C. Morieux, U. Kornak, J. Essig, E. Erxlebe, I. Bab, C. Kubisch, Cannabinoid receptor type 2 gene is associated with human osteoporosis, *Hum. Mol. Genet.*, 14 (2005) 3389-3396.
- [16] N.E. Campillo, J. Paez, Cannabinoid system in neurodegeneration: new perspectives in Alzheimer's disease, *Mini-Rev. Med. Chem.*, 9 (2009) 539-559.
- [17] M.A. Tabrizi, P.G. Baraldi, P.A. Borea, K. Varani, Medicinal chemistry, pharmacology, and potential therapeutic benefits of cannabinoid CB2 receptor agonists, *Chem. Rev.*, 116 (2016) 519-560.
- [18] S. Han, J.-J. Chen, J.-Z. Chen, Latest progress in the identification of novel synthetic ligands for the cannabinoid CB2 receptor, *Mini-Rev. Med. Chem.*, 14 (2014) 426-443.
- [19] S. Han, J. Thatte, D.J. Buzard, R.M. Jones, Therapeutic utility of cannabinoid receptor type 2 (CB2) selective agonists, *J. Med. Chem.*, 56 (2013) 8224-8256.
- [20] D. Riether, Selective cannabinoid receptor 2 modulators: a patent review 2009-present, *Expert Opin. Ther. Pat.*, 22 (2012) 495-510.
- [21] R.G. Pertwee, A. Howlett, M.E. Abood, S. Alexander, V. Di Marzo, M. Elphick, P. Greasley, H.S. Hansen, G. Kunos, K. Mackie, International Union of Basic and Clinical Pharmacology. LXXIX. Cannabinoid receptors and their ligands: beyond CB1 and CB2, *Pharmacol. Rev.*, 62 (2010) 588-631.
- [22] K.J. Valenzano, L. Tafesse, G. Lee, J.E. Harrison, J.M. Boulet, S.L. Gottshall, L. Mark, M.S. Pearson, W. Miller, S. Shan, L. Rabadi, Pharmacological and pharmacokinetic characterization of the cannabinoid receptor 2 agonist, GW405833, utilizing rodent models of acute and chronic pain, anxiety, ataxia and catalepsy, *Neuropharmacology*, 48 (2005) 658-672.
- [23] C. Lombard, M. Nagarkatti, P. Nagarkatti, CB2 cannabinoid receptor agonist, JWH-015, triggers apoptosis in immune cells: potential role for CB2-selective ligands as immunosuppressive agents, *Clin. Immunol.*, 122 (2007) 259-270.
- [24] M.M. Ibrahim, H. Deng, A. Zvonok, D.A. Cockayne, J. Kwan, H.P. Mata, T.W. Vanderah, J. Lai, F. Porreca, A. Makriyannis, Activation of CB2 cannabinoid receptors by AM1241 inhibits experimental neuropathic pain: pain inhibition by receptors not present in the CNS, *Proc. Natl. Acad. Sci. USA*, 100 (2003) 10529-10533.
- [25] H. Iwamura, H. Suzuki, Y. Ueda, T. Kaya, T. Inaba, In vitro and in vivo pharmacological characterization of JTE-907, a novel selective ligand for cannabinoid CB2 receptor, *J. Pharmacol. Exp. Ther.*, 296 (2001) 420-425.
- [26] T. Maekawa, H. Nojima, Y. Kuraishi, K. Aisaka, The cannabinoid CB2 receptor inverse agonist JTE-907 suppresses spontaneous itch-associated responses of NC mice, a model of atopic dermatitis, *Eur. J. Pharmacol.*, 542 (2006) 179-183.
- [27] G.M. Giblin, C.T. O'Shaughnessy, A. Naylor, W.L. Mitchell, A.J. Eatherton, B.P. Slingsby, D.A. Rawlings, P. Goldsmith, A.J. Brown, C.P. Haslam, Discovery of 2-[(2,4-dichlorophenyl)amino]-N-[(tetrahydro-2H-pyran-4-yl)methyl]-4-(trifluoromethyl)-5-pyrimidinecarboxamide, a selective CB2 receptor agonist for the treatment of inflammatory pain, *J. Med. Chem.*, 50 (2007) 2597-2600.
- [28] GlaxoSmithKline, Dental pain 3rd molar tooth extraction GW842166, <https://clinicaltrials.gov/ct2/show/NCT00444769>. Identifier: NCT00444769.
- [29] M. Odan, N. Ishizuka, Y. Hiramatsu, M. Inagaki, H. Hashizume, Y. Fujii, S. Mitsumori, Y. Morioka, M. Soga, M. Deguchi, Discovery of S-777469: an orally available CB2 agonist as an antipruritic agent, *Bioorg. Med. Chem.*

Let., 22 (2012) 2803-2806.

[30] T. Haruna, M. Soga, Y. Morioka, I. Hikita, K. Imura, Y. Furue, M. Yamamoto, C. Imura, M. Ikeda, A. Yamauchi, S-777469, a Novel Cannabinoid Type 2 Receptor Agonist, Suppresses Itch-Associated Scratching Behavior in Rodents through Inhibition of Itch Signal Transmission,, *Pharmacology*, 95 (2015) 95-103.

[31] Shionogi Inc., A randomized, double-blind study to evaluate the safety and efficacy of 2 doses of S-777469 in patients with atopic dermatitis., <https://clinicaltrials.gov/ct2/show/NCT00703573>. Identifier: NCT00703573.

[32] C. Mugnaini, A. Brizzi, A. Ligresti, M. Allarà, S. Lamponi, F. Vacondio, C. Silva, M. Mor, V. Di Marzo, F. Corelli, Investigations on the 4-quinolone-3-carboxylic acid motif. 7. Synthesis and pharmacological evaluation of 4-quinolone-3-carboxamides and 4-hydroxy-2-quinolone-3-carboxamides as high affinity cannabinoid receptor 2 (CB2R) Ligands with Improved Aqueous Solubility *J. Med. Chem.*, 59 (2016) 1052-1067.

[33] H.-Y. Qian, Z.-L. Wang, Y.-L. Pan, L.-L. Chen, X. Xie, J.-Z. Chen, Development of quinazoline/pyrimidine-2,4(1*H*,3*H*)diones as agonists of cannabinoid receptor type 2, *ACS Med. Chem. Lett.*, (2017) DOI: 10.1021/acsmchemlett.7b00007.

[34] B.A. Ellsworth, P.M. Sher, X. Wu, G. Wu, R.B. Sulsky, Z. Gu, N. Murugesan, Y. Zhu, G. Yu, D.F. Sitkoff, K.E. Carlson, L. Kang, Y. Yang, N. Lee, R.A. Baska, W.J. Keim, M.J. Cullen, A.V. Azzara, E. Zuvich, M.A. Thomas, K.W. Rohrbach, J.J. Devenny, H.E. Godonis, S.J. Harvey, B.J. Murphy, G.G. Everlof, P.I. Stetsko, O. Gudmundsson, S. Johnghar, A. Ranasinghe, K. Behnia, M.A. Pelleymounter, W.R. Ewing, Reductions in log P improved protein binding and clearance predictions enabling the prospective design of cannabinoid receptor (CB1) antagonists with desired pharmacokinetic properties, *J. Med. Chem.*, 56 (2013) 9586-9600.

[35] W.L. Mitchell, G.M. Giblin, A. Naylor, A.J. Eatherton, B.P. Slingsby, A.D. Rawlings, K.S. Jandu, C.P. Haslam, A.J. Brown, P. Goldsmith, Pyridine-3-carboxamides as novel CB2 agonists for analgesia, *Bioorg. Med. Chem. Lett.*, 19 (2009) 259-263.

[36] R.J. Gleave, P.J. Beswick, A.J. Brown, G.M. Giblin, P. Goldsmith, C.P. Haslam, W.L. Mitchell, N.H. Nicholson, L.W. Page, S. Patel, Synthesis and evaluation of 3-amino-6-aryl-pyridazines as selective CB 2 agonists for the treatment of inflammatory pain, *Bioorg. Med. Chem. Lett.*, 20 (2010) 465-468.

[37] T. Zhu, L.-Y. Fang, X. Xie, Development of a universal highthroughput calcium assay for G-protein-coupled receptors with promiscuous G-protein G α 15/16, *Acta Pharmacol. Sin.*, 29 (2008) 507-516.

[38] S. Hussain, A. Khan, S. Gul, M. Resmini, C.S. Verma, E.W. Thomas, K. Brocklehurst, Identification of interactions involved in the generation of nucleophilic reactivity and of catalytic competence in the catalytic site Cys/His ion pair of papain, *Biochemistry*, 50 (2011) 10732-10742.

[39] S. Konno, M. Sagi, F. Siga, H. Yamanaka, Synthesis of 6-alkylamino-3-pyridazinecarboxylic acid derivatives from methyl 6-chloro-3-pyridazine-carboxylate, *Heterocycles*, 34 (1992) 225-228.

[40] Y. Uto, Y. Kiyotsuka, Y. Ueno, Y. Miyazawa, H. Kurata, T. Ogata, T. Deguchi, M. Yamada, N. Watanabe, M. Konishi, Novel spiropiperidine-based stearyl-CoA desaturase-1 inhibitors: Identification of 1'-{6-[5-(pyridin-3-ylmethyl)-1,3,4-oxadiazol-2-yl]pyridazin-3-yl}-5-(trifluoromethyl)-3,4-dihydrospiro-[chromene-2,4'-piperidine], *Bioorg. Med. Chem. Lett.*, 20 (2010) 746-754.

[41] A. Volonterio, L. Moisan, J. Rebek, Synthesis of pyridazine-based scaffolds as α -helix mimetics, *Org. Lett.*, 9 (2007) 3733-3736.

[42] R.E. Hackler, W.R. Arnold, W.C. Dow, G.W. Johnson, S.V. Kaster, Structure-activity relationships in (haloalkyl) pyridazines: a new class of systemic fungicides, *J. Agric. Food Chem.*, 38 (1990) 508-514.

[43] C. Lunniss, C. Eldred, N. Aston, A. Craven, K. Gohil, B. Judkins, S. Keeling, L. Ranshaw, E. Robinson, T. Shipley, Addressing species specific metabolism and solubility issues in a quinoline series of oral PDE4 inhibitors, *Bioorg. Med. Chem. Lett.*, 20 (2010) 137-140.

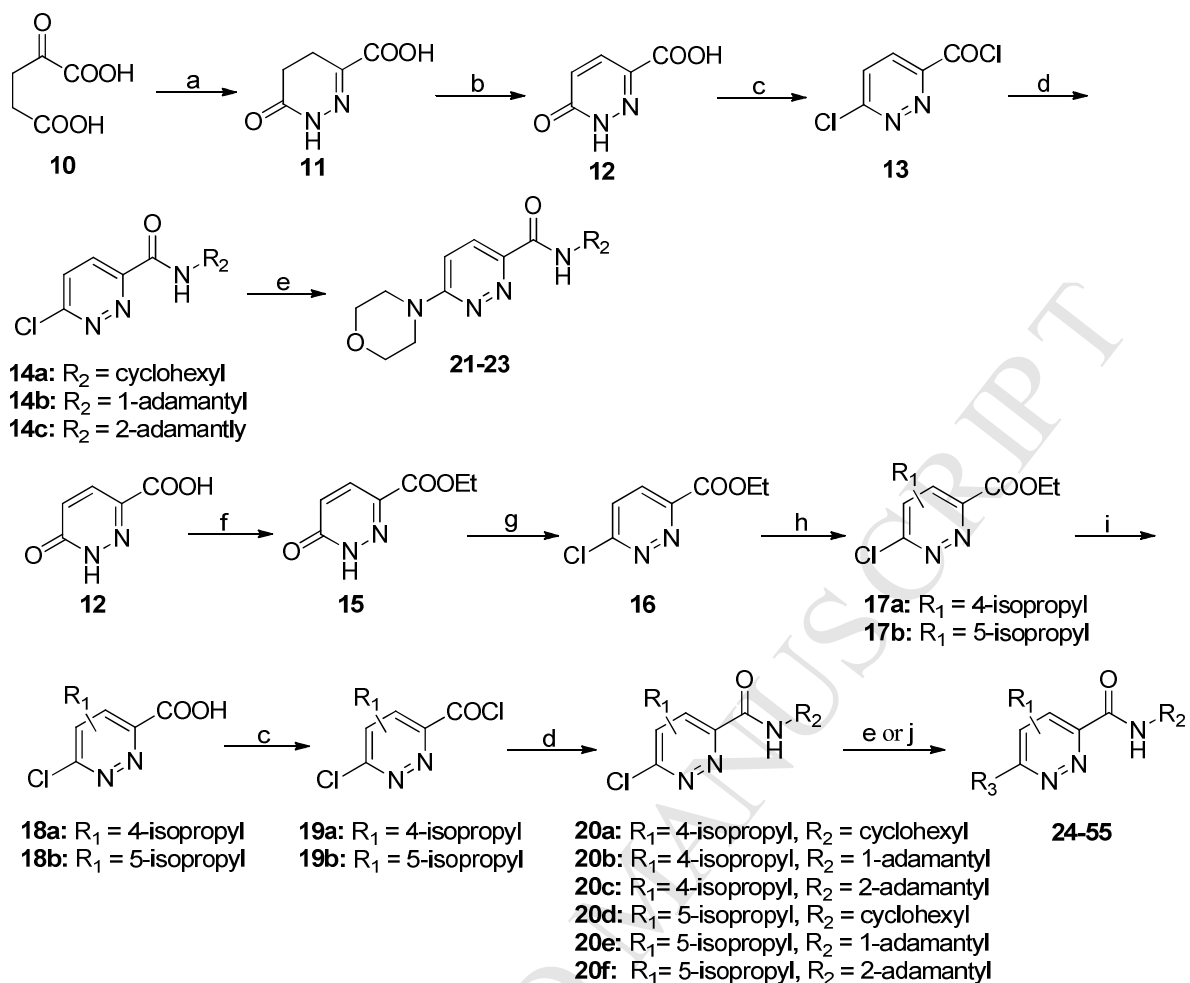
[44] B.B. Yao, G.C. Hsieh, J.M. Frost, Y. Fan, T.R. Garrison, A.V. Daza, G.K. Grayson, C.Z. Zhu, M. Pai, P. Chandran,

- A.K. Salyers, E.J. Wensink, P. Honore, J.P. Sullivan, M.J. Dart, M.D. Meyer, In vitro and in vivo characterization of A-796260: a selective cannabinoid CB2 receptor agonist exhibiting analgesic activity in rodent pain models, *Br. J. Pharmacol.*, 153 (2008) 390-401.
- [45] ACD/ADME Suite, version 5, Advanced Chemistry Development, Inc., in, 110 Yonge Street, Toronto, Ontario M5C 1T4, Canada.
- [46] T. Bohnert, C. Prakash, ADME Profiling in Drug Discovery and Development: An Overview, in: A.V. Lyubimov (Ed.) *Encyclopedia of Drug Metabolism and Interactions*, 6-Volume Set, John Wiley & Sons, Inc, 2012.
- [47] Sybyl Molecular Modeling Software Packages, version X1.3, Tripos Associates, St. Louis, MO63144, 2011.
- [48] S. Han, F.-F. Zhang, X. Xie, J.-Z. Chen, Design, synthesis, biological evaluation, and comparative docking study of 1, 2, 4-triazolones as CB1 receptor selective antagonists, *Eur. J. Med. Chem.*, 74 (2014) 73-84.
- [49] Z. Feng, M.H. Alqarni, P. Yang, Q. Tong, A. Chowdhury, L. Wang, X.-Q. Xie, Modeling, molecular dynamics simulation, and mutation validation for structure of cannabinoid receptor 2 based on known crystal structures of GPCRs, *J. Chem. Inf. Model.*, 54 (2014) 2483-2499.
- [50] E. Cichero, A. Ligresti, M. Allarà, V. di Marzo, Z. Lazzati, P. D'Ursi, A. Marabotti, L. Milanesi, A. Spallarossa, A. Ranise, Homology modeling in tandem with 3D-QSAR analyses: a computational approach to depict the agonist binding site of the human CB2 receptor, *Eur. J. Med. Chem.*, 46 (2011) 4489-4505.
- [51] M.H. Rhee, I. Nevo, M.L. Bayewitch, O. Zagoory, Z. Vogel, Functional role of tryptophan residues in the fourth transmembrane domain of the CB2 cannabinoid receptor, *J. Neurochem.*, 75 (2000) 2485-2491.
- [52] O.M. Salo, K.H. Raitio, J.R. Savinainen, T. Nevalainen, M. Lahtela-Kakkonen, J.T. Laitinen, T. Järvinen, A. Poso, Virtual screening of novel CB2 ligands using a comparative model of the human cannabinoid CB2 receptor, *J. Med. Chem.*, 48 (2005) 7166-7171.
- [53] S. Han, F.-F. Zhang, H.-Y. Qian, L.-L. Chen, J.-B. Pu, X. Xie, J.-Z. Chen, Development of quinoline-2,4(1H,3H)-diones as potent and selective ligands of the cannabinoid type 2 receptor, *J. Med. Chem.*, 58 (2015) 5751-5769.
- [54] V. Lucchesi, D.P. Hurst, D.M. Shore, S. Bertini, B.M. Ehrmann, M. Allara, L. Lawrence, A. Ligresti, F. Minutolo, G. Saccomanni, H. Sharir, M. Macchia, V. Di Marzo, M.E. Abood, P.H. Reggio, C. Manera, CB2-selective cannabinoid receptor ligands: synthesis, pharmacological evaluation, and molecular modeling investigation of 1,8-naphthyridin-2(1H)-one-3-carboxamides, *J. Med. Chem.*, 57 (2014) 8777-8791.
- [55] R.C. Evans, F.Y. Wiselogle, Studies in the pyridazine series. The absorption spectrum of pyridazine, *J. Am. Chem. Soc.*, 67 (1945) 60-62.
- [56] J.A. King, F.H. McMillan, The Preparation of Some Pyridazonyl Acids, *J. Am. Chem. Soc.*, 74 (1952) 3222-3224.

Figure captions:

Figure 1. Chemical structures of some representative cannabinoids and the scaffold of our synthesized pyridazine-3-carboxamides.

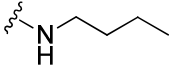
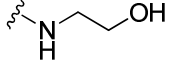
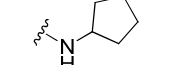
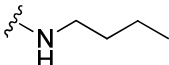
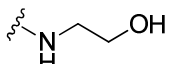
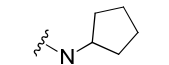
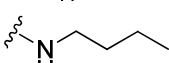
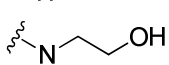
Figure 2. Docking results of CB2-agonist **26** (A), CB2-agonist **29** (B), CB2-agonist **37** (C), and CB2-agonist **38** (D) complexes. The carbon atoms of F117/W258 motif are shown in purple, and the H-bonds are illustrated by green dashed lines.



Scheme 1. Reagents and conditions: (a) $\text{NH}_2\text{NH}_2 \cdot \text{H}_2\text{SO}_4$, NaOH, H_2O , 105 °C, overnight; (b) AcOH, Br_2 , H_2O , reflux, overnight; (c) SOCl_2 , DMF, $\text{CH}_2\text{ClCH}_2\text{Cl}$, 68 °C, overnight; (d) R_2NH_2 , Et_3N , DCM, rt, overnight; (e) aliphatic amines, DIPEA, 1,4-dioxane, reflux, overnight; (f) EtOH, HCl, reflux, 14 h; (g) POCl_3 , 100 °C, 2 h; (h) $\text{R}_1\text{-COOH}$, $(\text{NH}_4)_2\text{S}_2\text{O}_8$, AgNO_3 , *conc.* H_2SO_4 , H_2O , 70-75 °C, 30 min; (i) LiOH, THF, H_2O , 0 °C, 30 min; (j) aromatic amines, DIPEA, CH_3CN , 92 °C to 160 °C.

Table 1. Agonist activities of compounds **21-38** in CHO cells expressing CB1 or CB2 receptor determined by calcium mobilization assays.

No.	R ₁	R ₂	R ₃	clogD ^a	clogS ^b	CB1 EC ₅₀ (nM)	CB2 EC ₅₀ ^c (95% CI, nM)	CB2 E _{max} ^d (% of control)	SI ^e
21	H	cyclohexyl		1.67	-2.38	>10000	>10000	-	-
22	H	1-adamantyl		2.72	-3.15	>10000	>10000	-	-
23	H	2-adamantyl		2.86	-2.60	>10000	8425 ± 4183	79 ± 5	>1
24	4-isopropyl	cyclohexyl		2.70	-2.79	>10000	594.0 ± 72.2	91 ± 1	>17
25	4-isopropyl	1-adamantyl		3.65	-3.45	>10000	396.2 ± 81.9	93 ± 4	>25
26	4-isopropyl	2-adamantyl		3.84	-2.88	>10000	3.665 ± 0.553	91 ± 10	>2729
27	5-isopropyl	cyclohexyl		2.98	-2.88	>10000	969.7 ± 148.3	99 ± 3	>10
28	5-isopropyl	1-adamantyl		3.76	-3.90	>10000	349.0 ± 34.2	125 ± 2	>29
29	5-isopropyl	2-adamantyl		3.74	-3.22	>10000	403.3 ± 13.4	105 ± 4	>25
30	4-isopropyl	cyclohexyl		4.10	-3.16	>10000	338.2 ± 53.3	78 ± 4	>30

31	4-isopropyl	cyclohexyl		4.01	-3.25	>10000	>10000	-	-
32	4-isopropyl	cyclohexyl		2.10	-2.08	>10000	841.9 ± 224.3	81 ± 4	>12
33	4-isopropyl	1-adamantyl		5.03	-4.18	>10000	301.0 ± 104.7	80 ± 8	>33
34	4-isopropyl	1-adamantyl		4.75	-4.02	10000	159.4 ± 37.9	76 ± 5	>63
35	4-isopropyl	1-adamantyl		3.16	-2.86	>10000	42.64 ± 2.66	114 ± 2	>235
36	4-isopropyl	2-adamantyl		4.87	-3.32	>10000	5.701 ± 1.993	107 ± 5	>1754
37	4-isopropyl	2-adamantyl		4.71	-3.51	>10000	49.35 ± 8.98	108 ± 4	>203
38	4-isopropyl	2-adamantyl		3.26	-2.41	>10000	4.955 ± 0.633	94 ± 9	>2018
GW842166X				4.66	-5.65	>10000	342.8 ± 46.4	97 ± 2	>29
CP55940				6.24	-5.27	30.02 ± 8.40	28.62 ± 6.42	100 ± 8	1.6

^aclogD: Calculated at PH = 7.4 using ADME Suite 5.0 (ACD/Labs).

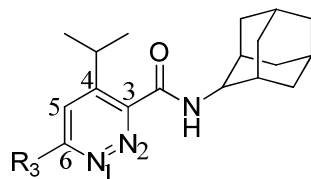
^bclogS: Calculated in buffer at PH = 7.4 using ADME Suite 5.0 (ACD/Labs).

^cData represent mean values ± SEM of eight-point experiments each performed in triplicate. CI, confidence interval.

^dE_{max} displayed as mean values ± SEM are relative (%) to the maximal effect of **CP55940**.

^eSI: selectivity index for the CB2 receptor, SI = EC₅₀(CB1)/EC₅₀(CB2).

Table 2. Agonist activities of compounds **39-45** in CHO cells expressing CB1 or CB2 receptor determined by calcium mobilization assays.



No.	R ₃	clogD ^a	clogS ^b	CB1 EC ₅₀ (nM)	CB2 EC ₅₀ ^c (95% CI, nM)	CB2 E _{max} ^d (% of control)	SI ^e
39		4.65	-3.58	>10000	18.08 ± 2.89	140 ± 0.5	>553
40		3.08	-1.95	>10000	>10000	-	-
41		5.22	-3.53	>10000	398.2 ± 164.9	81 ± 1	>25
42		4.42	-3.66	>10000	17.13 ± 1.59	117 ± 3	>584
43		4.66	-3.89	>10000	47.68 ± 6.63	135 ± 7	>210
44		5.04	-3.79	>10000	2940 ± 1123	77 ± 4	>3
45		5.71	-4.73	>10000	6699 ± 2838	77 ± 5	>1

^aclogD: Calculated at PH = 7.4 using ADME Suite 5.0 (ACD/Labs).

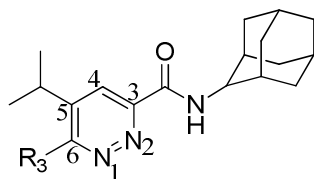
^bclogS: Calculated in buffer at PH = 7.4 using ADME Suite 5.0 (ACD/Labs).

^cEC₅₀ values were obtained from one experiment with three replicates. CI, confidence interval.

^dE_{max} displayed as mean values ± SEM are relative (%) to the maximal effect of **CP55940**.

^eSI: selectivity index for the CB2 receptor, SI = EC₅₀(CB1)/EC₅₀(CB2).

Table 3. Agonist activities of compounds **46-55** in CHO cells expressing CB1 or CB2 receptor determined by calcium mobilization assays.



No.	R ₃	clogD ^a	clogS ^b	CB1 EC ₅₀ (nM)	CB2 EC ₅₀ ^c (95% CI, nM)	CB2 E _{max} ^d (% of control)	SI ^e
46		4.69	-3.95	>10000	3453 ± 203	106 ± 1	>3
47		5.27	-3.70	>10000	198.8 ± 25.4	91 ± 4	>50
48		4.87	-3.46	>10000	34.42 ± 2.97	114 ± 4	>291
49		4.66	-4.18	6047 ± 2338	167.0 ± 10.4	109 ± 7	36
50		4.73	-3.92	2605 ± 567	96.24 ± 17.98	93 ± 6	27
51		5.35	-4.18	>10000	>10000	-	-
52		3.17	-2.61	>10000	99.86 ± 21.14	127 ± 10	>100
53		5.63	-4.95	>10000	>10000	-	-

^aclogD: Calculated at PH = 7.4 using ADME Suite 5.0 (ACD/Labs).

^bclogS: Calculated in buffer at PH = 7.4 using ADME Suite 5.0 (ACD/Labs).

^cEC₅₀ values were obtained from one experiment with three replicates. CI, confidence interval.

^dE_{max} displayed as mean values ± SEM are relative (%) to the maximal effect of **CP55940**.

^eSI: selectivity index for the CB2 receptor, SI = EC₅₀(CB1)/EC₅₀(CB2).

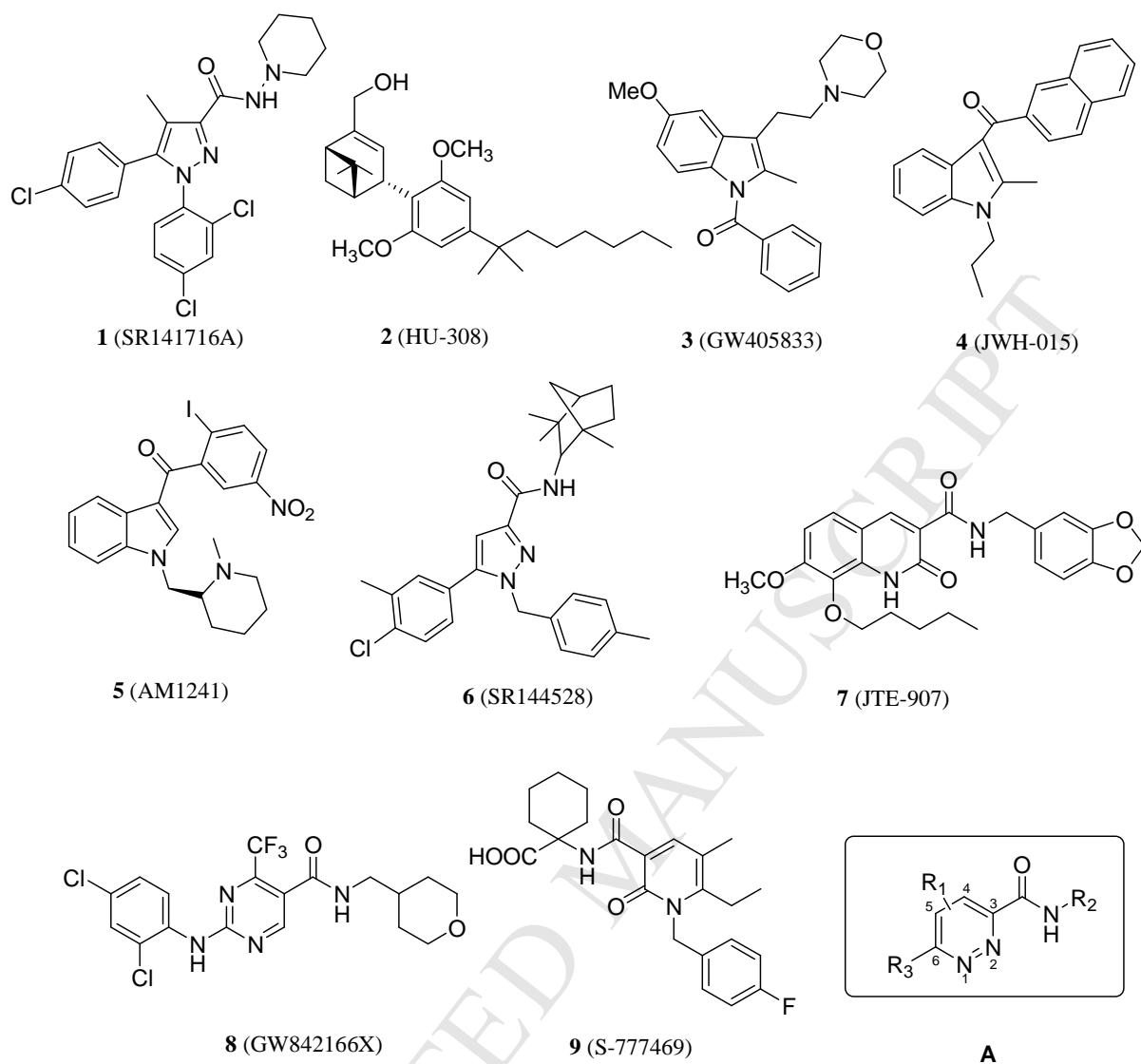


Figure 1. Some representative cannabinoids and the scaffold of our synthesized pyridazine-3-carboxamides.

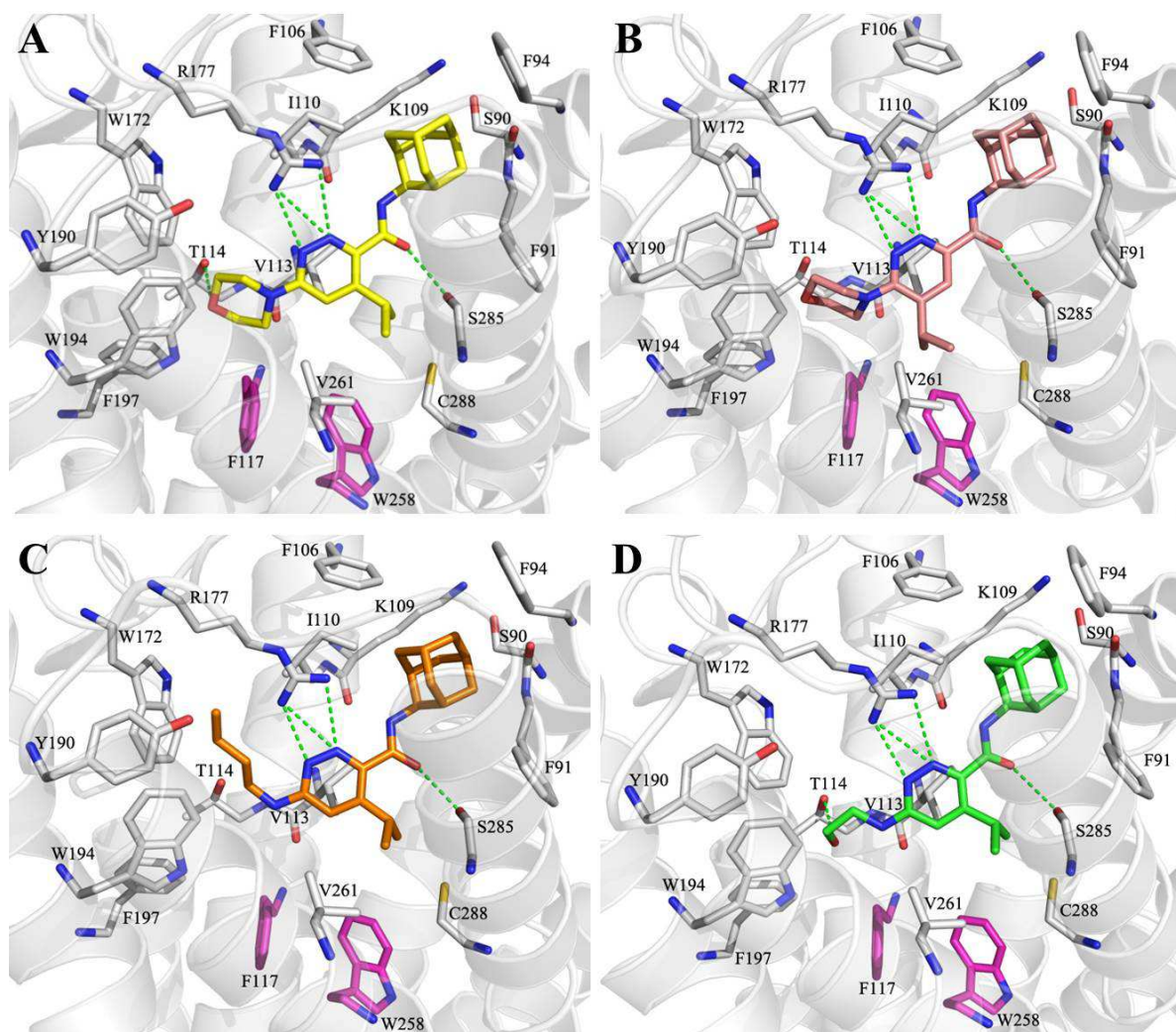


Figure 2. Docking results of CB2-agonist **26** (A), CB2-agonist **29** (B), CB2-agonist **37** (C), and CB2-agonist **38** (D) complexes. The carbon atoms of F117/W258 motif are shown in purple, and the H-bonds are illustrated by green dashed lines.

- Novel pyridazine-3-carboxamides were designed and synthesized to be CB2 agonists.
- Drug-likenesses of compounds demonstrated to be improved by measuring logP
- Dockings were performed to predict interaction modes of compounds binding to CB2.
- SARs were studied to imply pharmacophore features for pyridazine-3-carboxamides.